DENSITY AND STRESS DISTRIBUTION IN THE MOON*

JAFAR ARKANI-HAMED**
Lunar Science Institute, Houston, Tex., U.S.A.†

(Received 12 October, 1972)

Abstract. A model is presented for the lateral variations of density within the Moon. The model gives rise to a gravitational potential which is equal to the observed potential at the lunar surface, moreover, it minimizes the total shear-strain energy of the Moon. The model exhibits lateral variations of about ± 0.25 g cc^{-1} within 50 km depth. The variations, however, reduce to ± 0.06 and ± 0.008 g cc^{-1} within layers at 50–135 and 135–235 km respectively, and they become negligible below this region. The associated stress differences are found to be about 50 bar within 600 km depth, having their maximum values of about 90 bars at a depth of about 250 km. On the basis of these stress differences a strength of about 100 bar is concluded for the upper 400 km of the lunar interior for the last 3.3 b.y.

0. Introduction

In a previous paper (Arkani-Hamed, 1973a), called hereafter Paper I, a model was determined for the lateral density variations of the Moon. The variations were confined to a surface layer of 50 km thickness and the associated stress differences were found to be on the order of 40 bar within 800 km depth (they obtained maximum values of about 70 bar at about 180 km depth). The paper meant to present preliminary results of the research which was being carried out. In the present paper, however, we are concerned with the final results of the research. Here a model is presented for the lateral variations of density inside the whole Moon. The model gives rise to a gravitational potential which is equal to the observed potential at the lunar surface. Moreover it minimizes the associated shear-strain energy of the Moon.

The first section is devoted to the correlation of different spherical harmonic expressions suggested for the observed lunar gravitational potential. In the second section a formula is developed for the determination of the lateral density perturbations through the elastic deformation equations. A reader familiar with this procedure may pass this section. On the basis of this formula a most reliable density model is obtained in the following section. The associated stress differences are calculated in section four. The effects of different phenomena, such as the topography of the lunar surface, on the density perturbations are discussed in the fifth section, and a final density model as well as its geophysical implications are also presented in this section.

It is worthwhile to point out that throughout this paper the attention is focused on the front side of the Moon where most of the gravitational data come from. Therefore, the results of this investigation are valid on the front side.

* Paper dedicated to Professor Harold C. Urey on the occasion of his 80th birthday on 29 April, 1973.
** Permanent address: Dept. of Physics, Arya-Mehr University of Technology, Tehran, Iran.
† The Lunar Science Institute is operated by the Universities Space Research Association under Contract No. NSR 09-051-001 with the National Aeronautics and Space Administration. This paper is Lunar Science Institute Contribution No. 117.

The Moon 7 (1973) 84–126.

1. Data Correlation

Different expressions have been suggested for the gravitational potential of the Moon (Lorell and Sjogren, 1967; Lorell, 1969; Michael *et al.*, 1969; Michael and Blackshear, 1971). To illustrate the existence or lack of any agreement among these expressions we determine a cumulative correlation coefficient between any two sets of them. The cumulative correlation coefficient, η_N, is defined as

$$\eta_N = \frac{\sum_{n=2}^{N} \sum_{m=0}^{n} (A_{nm}A'_{nm} + B_{nm}B'_{nm})}{\left[\sum_{n=2}^{N} \sum_{m=0}^{n} (A_{nm}^2 + B_{nm}^2)\right]^{1/2} \left[\sum_{n=2}^{N} \sum_{m=0}^{n} A'^2_{nm} + B'^2_{nm}\right]^{1/2}}, \tag{1}$$

where n and m are the degree and the order of a spherical harmonic, (A_{nm}, B_{nm}) are the fully normalized spherical harmonic coefficients of one set and (A'_{nm}, B'_{nm}) are those of the other set. A fully normalized spherical harmonic $S_{nm}(\theta, \varphi)$ is defined so that

$$\int_0^{2\pi} \mathrm{d}\varphi \int_0^{\pi} \sin\theta \, \mathrm{d}\theta \, S^*_{nm} \cdot S_{kl} = 4\pi \delta_{nk} \delta_{ml}, \tag{2}$$

where θ=colatitude, φ=longitude, and δ_{nK}=Kronecker's delta function. Table I shows the cumulative correlation coefficients obtained through Equation (1) for a value of N equals to 4. It is clear from the table that the expressions tend to agree at the low degree harmonics. These coefficients, however, are probably biased because all of the expressions are based on data from the front side of the Moon, primarily. Any low degree harmonic density variations of the back side would affect the gravitational potential of the front side (Paper I). Therefore, the low degree harmonics alone are not appropriate to be used in determining the lateral variations of density in the front side.

TABLE I

Correlation coefficients between six different spherical harmonic presentations of the lunar gravitational potential. G_1 = Lorell and Sjogren, 1967; G_2, G_3 and G_4 = Lorell, 1969; G_5 = Michael *et al.*, 1969; G_6 = Michael and Blackshear, 1971

	G_1	G_2	G_3	G_4	G_5	G_6
G_1	1					
G_2	0.715	1				
G_3	0.596	0.795	1			
G_4	0.556	0.779	0.792	1		
G_5	0.637	0.784	0.729	0.767	1	
G_6	0.738	0.837	0.840	0.800	0.929	1

G_5 and G_6 are the expressions which include the higher degree harmonics. Since any plausible high degree harmonic density variations of the back side do not contri-

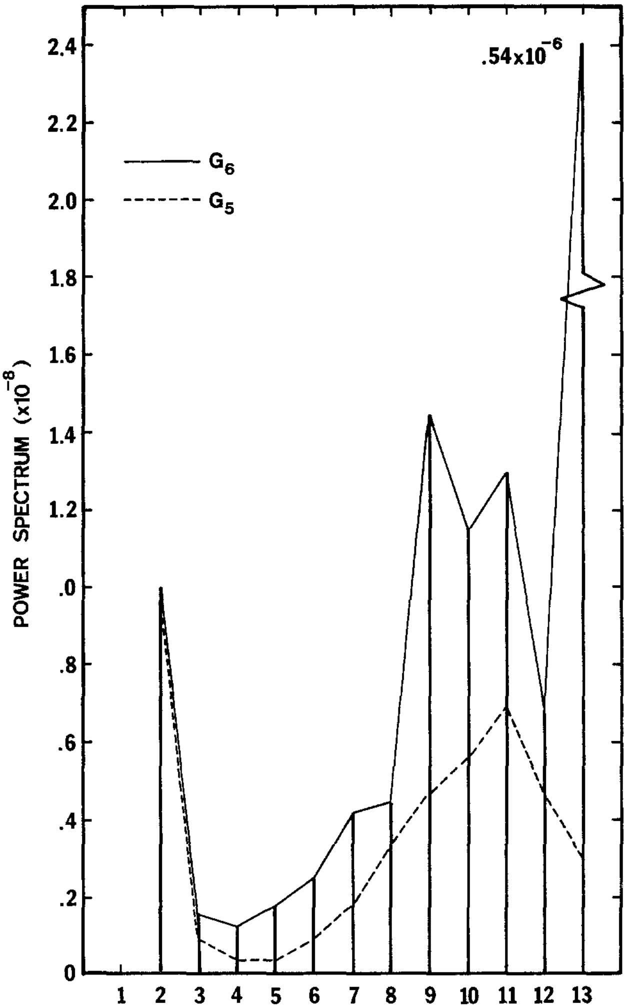

Fig. 1. Degree power spectrum of two expressions for the lunar gravitational potentials, G_5 and G_6. Units are in $(\Phi_0)^2$ where Φ_0 = gravitational potential at the surface of the initial model

bute to the gravitational potential on the front side significantly (Paper I), these two expressions are probably informative about the short wave length density variations (such as mascons) of the front side. Figure 1 illustrates the degree power spectrum, σ_n, of these expressions where σ_n is determined from

$$\sigma_n = \sum_{m=0}^{n} (A_{nm}^2 + B_{nm}^2). \tag{3}$$

The general behavior of G_5 and G_6 are similar except for the 13th degree harmonics. It is clear from the figure that aside from the second degree harmonics which are strongly affected by the bulge of the Moon, the gravitational potential of the Moon is characterized by the high degree harmonics. Figure 2 shows the degree correlation

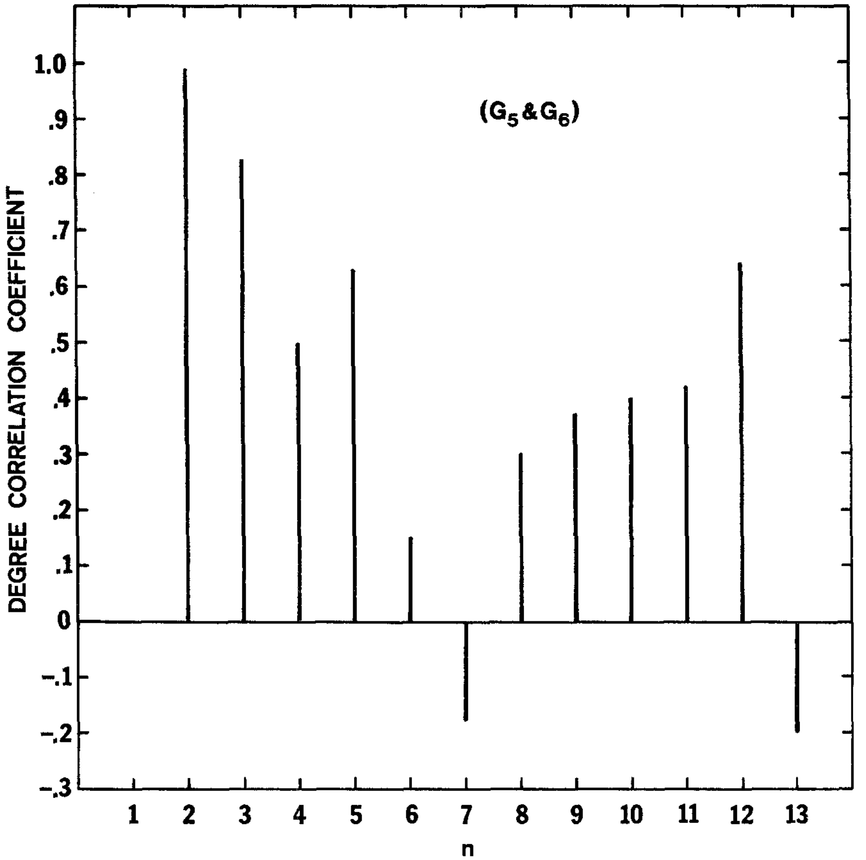

Fig. 2. Degree correlation coefficients of G_5 and G_6.

coefficient, γ_n, between G_5 and G_6, where γ_n is computed through

$$\gamma_n = \frac{\sum\limits_{m=0}^{n} (A_{nm}A'_{nm} + B_{nm}B'_{nm})}{\left[\sum\limits_{m=0}^{n} (A_{nm}^2 + B_{nm}^2)\right]^{1/2} \left[\sum\limits_{m=0}^{n} (A'^2_{nm} + B'^2_{nm})\right]^{1/2}}. \tag{4}$$

In general, the low degree harmonics correlate better than the high degree ones. A very small positive correlation coefficient of the 6th degree harmonics and a negative correlation coefficient of the 7th degree harmonics imply some uncertainty in the spherical harmonic coefficients of the higher degree harmonics. However, the cumulative correlation coefficients of G_5 and G_6 (Figure 3) are not affected strongly by the degree correlation coefficients of the 6th and 7th degree harmonics. The cumulative correlation coefficients are generally high, $\geqslant 0.5$, except when the 13th degree harmonics are taken into account, in which case the coefficient reduces to about 0.1. The foregoing quantities lead us to conclude that there is an overall agreement between G_5 and G_6 for the harmonics through the 12th degree.

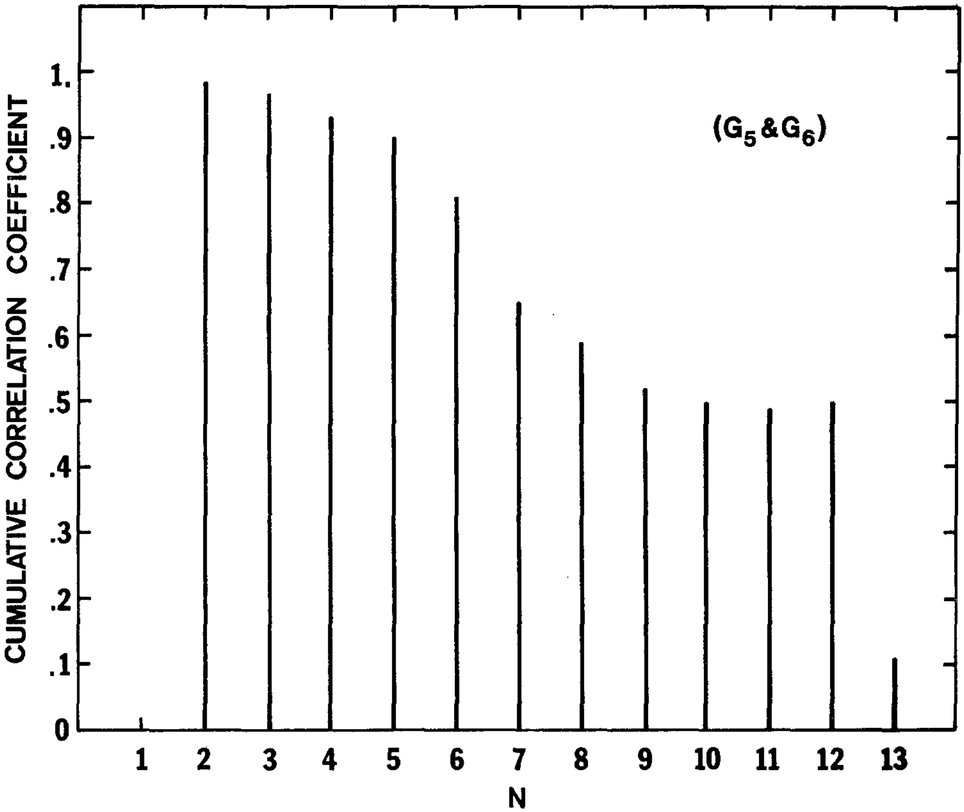

Fig. 3. Cumulative correlation coefficients of G_5 and G_6.

G_5 is the expression which we adopted for the gravitational potential of the Moon in Paper I. In the present paper, however, we use G_6 because it is a new expression and it is based on almost twice as much data as G_5 (Michael and Blackshear, 1971). Table II shows the fully normalized spherical harmonic coefficients of G_6. The 13th degree harmonics are excluded in the present studies because they exhibit very abnormal characteristics in the two expressions. Such a behavior is also evident from the degree power spectrum ratio; the degree power spectrum of G_6 divided by that of G_5, which is illustrated in Figure 4. The ratios are less than 5 for all of the harmonics except the 13th degree ones in which case the ratio is about 180.

2. Theory

In this section we present the final formula through which the lateral variations of density inside the lunar interior are calculated. The formula is derived from the solution of the equilibrium equations together with the minimization of the total shear strain energy in the Moon.

TABLE II

Fully normalized spherical harmonic coefficients of the lunar gravitational potential presented by Michael and Blackshear, 1971. Units are in ergs. Odd denotes their S_{nm} terms while even denotes their C_{nm} terms

n	m	Odd	Even	n	m	Odd	Even
2	0	.00000000	.00000000	9	2	−.12940000+006	−.18030000+006
2	1	.28470000+006	.24190000+006	9	3	−.20530000+006	−.48270000+006
2	2	−.45720000+003	.10880000+007	9	4	.70140000+006	−.27600000+006
3	0	.00000000	.30380000+006	9	5	−.69410000+006	.24110000+006
3	1	.54430000+006	.63190000+006	9	6	.26790000+006	−.11020000+007
3	2	.18790000+006	.63140000+006	9	7	.11970000+007	−.11960000+007
3	3	−.63080000+005	.28600000+006	9	8	.23070000+007	−.10940000+006
4	0	.00000000	.32670000+006	9	9	−.19940000+006	.65310000+006
4	1	−.25350000+006	−.59250000+006	10	0	.00000000	−.12050000+006
4	2	−.52640000+006	−.32150000+006	10	1	.20640000+005	.16300000+007
4	3	−.13090000+006	−.26630000+006	10	2	.27170000+006	.23380000+004
4	4	.15260000+006	−.72200000+005	10	3	−.17660000+006	−.10840000+005
5	0	.00000000	−.22680000+006	10	4	.54070000+006	.18780000+006
5	1	−.30540000+006	−.24730000+006	10	5	−.96990000+006	.17340000+006
5	2	.67680000+005	.60420000+005	10	6	.63720000+006	−.18830000+006
5	3	.75940000+006	.34250000+006	10	7	−.52170000+006	.92710000+006
5	4	−.53690000+006	.34090000+006	10	8	−.99930000+006	.13540000+007
5	5	−.24100000+006	.21540000+006	10	9	−.54960000+006	.14050000+006
6	0	.00000000	.38930000+006	10	10	.22540000+006	−.51160000+006
6	1	−.34360000+006	−.66600000+006	11	0	.00000000	.30070000+006
6	2	.41200000+005	−.12510000+006	11	1	.13630000+007	−.37000000+006
6	3	−.16140000+006	.15920000+006	11	2	.39570000+006	−.17610000+006
6	4	−.72430000+006	−.25350000+006	11	3	.34290000+006	.14310000+006
6	5	.28440000+006	−.33910000+006	11	4	.88630000+006	.69040000+005
6	6	.36070000+006	−.49470000+006	11	5	−.62930000+006	−.22640000+006
7	0	.00000000	−.53100000+006	11	6	.90080000+006	.44860000+006
7	1	−.10970000+007	.16140000+006	11	7	−.11020000+007	−.94920000+005
7	2	−.21040000+006	−.23660000+006	11	8	.16910000+006	−.57430000+006
7	3	−.35130000+006	−.25550000+006	11	9	.11800000+007	−.13110000+007
7	4	−.33810000+005	−.55470000+006	11	10	.60950000+006	−.44300000+006
7	5	.87110000+006	.14900000+006	11	11	−.16570000+006	.10190000+006
7	6	−.28920000+006	.18830000+006	12	0	.00000000	.55170000+005
7	7	−.18890000+006	.52300000+006	12	1	.72070000+005	.63780000+006
8	0	.00000000	−.11930000+006	12	2	.33170000+006	−.95420000+005
8	1	.15100000+006	.56340000+006	12	3	.66660000+005	.40970000+005
8	2	.31440000+006	.14040000+006	12	4	.11600000+006	.36490000+006
8	3	−.54110000+006	.26250000+005	12	5	−.51360000+006	.10090000+006
8	4	.54250000+006	−.13970000+006	12	6	.71660000+005	.20370000+006
8	5	−.14320000+006	.70290000+006	12	7	−.70840000+006	−.91950000+005
8	6	−.10550000+007	.36860000+006	12	8	.12410000+007	.15800000+006
8	7	.11930000+006	−.82340000+005	12	9	−.28420000+006	−.43480000+006
8	8	.26460000+006	−.79830000+006	12	10	−.10060000+007	.94090000+006
9	0	.00000000	−.42150000+006	12	11	−.27550000+006	.33430000+006
9	1	−.22730000+006	.23380000+005	12	12	.14340000+005	−.75090000+004

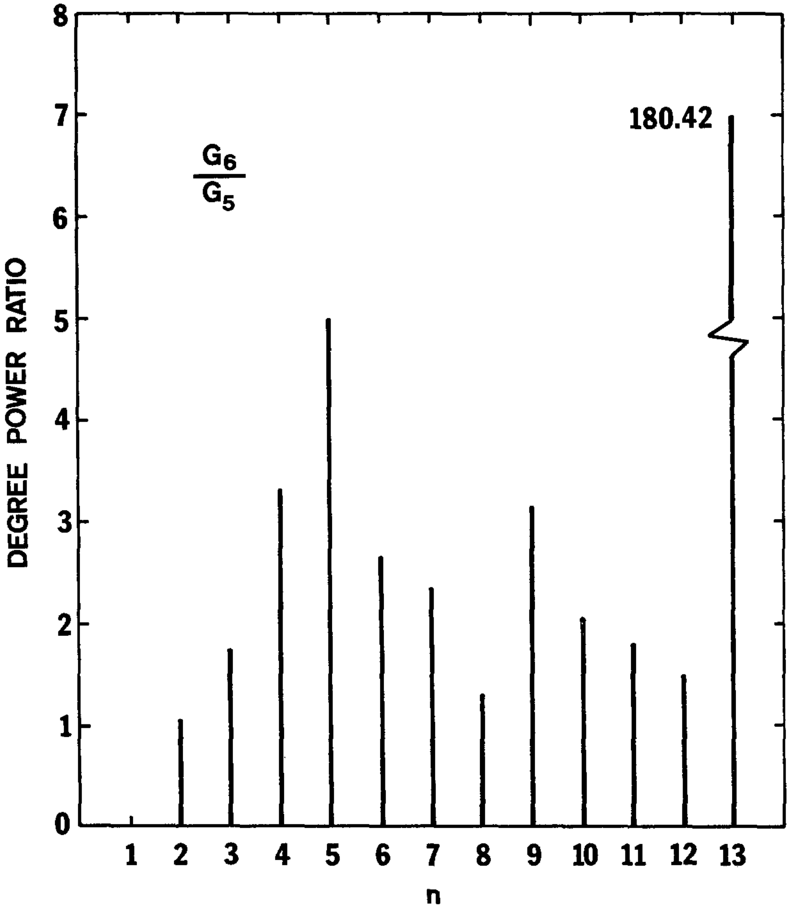

Fig. 4. Degree power ratios, the degree power of G_6 divided by that of G_5.

A. EQUILIBRIUM EQUATIONS

Here we review the derivation of the equilibrium equations for a self-gravitating and laterally heterogeneous lunar model. To construct such a model we start with a spherically symmetric initial model and introduce lateral perturbations of density into it. Then, we let the initial model deform under the perturbations due to its self-gravitational forces. The resulting model will be a laterally heterogeneous one in its equilibrium state. The equations to be presented describe this equilibrium state. The following assumptions and contraint are made throughout the derivation.

(1) The initial model is a gravitating and spherically symmetric body with no rotational motion. It is isotropic with linearly elastic interior.

(2) The stresses inside the initial model are purely hydrostatic with negligible thermal stresses.

(3) The deformation of the model specified by a first order perturbation from the

initial model. The perturbation does not affect the elastic moduli, but it changes density at a given location by means of dilatation and displacement.

The basic equations pertinent for this problem are:

(1) Conservation of momentum,

$$\nabla \cdot \bar{\bar{T}} + \bar{F} = 0, \tag{5}$$

where ∇ = gradient operator, $\bar{\bar{T}}$ = stress tensor, and $\bar{F}$ = gravitational body force acting on a unit volume, i.e.,

$$\bar{F} = -\varrho \nabla \Phi, \tag{6}$$

where ϱ = density and Φ = gravitational potential,

(2) Infinitesimal deformation equation,

$$\bar{\bar{E}} = \tfrac{1}{2}[\nabla \bar{u} + (\nabla \bar{u})^T], \tag{7}$$

where $\bar{\bar{E}}$ = strain tensor, $\bar{u}$ = displacement vector, and $(\nabla \bar{u})^T$ = transpose of $(\nabla \bar{u})$.

(3) Stress-strain relationship in an isotropic and a linearly elastic medium with the hydrostatic initial stresses,

$$\bar{\bar{T}} = [(\nabla \cdot \bar{u})\lambda - p_0 + \bar{u} \cdot \nabla p_0]\,\bar{\bar{I}} + 2\mu \bar{\bar{E}}, \tag{8}$$

where λ = Lamé constant, p_0 = initial hydrostatic pressure, $\bar{\bar{I}}$ = identity matrix, and μ = rigidity,

(4) Density at a given point after deformation, ϱ;

$$\varrho = \varrho_0 + \nabla \cdot (\varrho_0 \bar{u}) + \delta\varrho, \tag{9}$$

where ϱ_0 = density of the initial model, and $\delta\varrho$ = perturbations of the density which are introduced into the initial model. The second term in the right hand side specifies the density changes due to the deformation of the initial model.

(5) Poisson's equation for the gravitational potential,

$$\nabla^2 \Phi = -4\pi G \varrho, \tag{10}$$

where ∇^2 = Laplacian operator, and G = Newton's gravitational constant. The gravitational potential can be written as

$$\Phi = \Phi_0 + \psi, \tag{11}$$

where Φ_0 = gravitational potential of the initial model and ψ = perturbations of the gravitational potential due to the presence of $\delta\varrho$ and the deformation of the initial model. Using Equations (9) through (11) we express ψ as

$$\nabla^2 \psi = 4\pi G (\nabla \cdot (\varrho_0 \bar{u}) - \delta\varrho). \tag{12}$$

Putting Equations (6) through (12) into Equation (5) and neglecting the second order terms in $\bar{u}$ Equation (5) obtains the following form

$$\nabla \cdot [\lambda (\nabla \cdot \bar{u})\,\bar{\bar{I}} + \mu(\nabla \bar{u} + (\nabla u)^T)] + \varrho_0 \nabla \psi + \nabla (\bar{u} \cdot \nabla p_0) - \\ - [\nabla (\varrho_0 \bar{u}) - \delta\varrho]\,\nabla \Phi_0 = 0. \tag{13}$$

Equations (12) and (13) are four equations to be solved simultaneously.

We consider Equations (12) and (13) in a spherical coordinate system with origin at the center of the initial model. In such a coordinate system the lateral variation of density and the perturbations of the gravitational potential can be expressed in terms of spherical harmonics as

$$\delta\varrho(r,\theta,\varphi)=\sum_{nm}\Delta\varrho_{nm}(r)\,S_{nm}(\theta,\varphi), \tag{14}$$

and

$$\psi(r,\theta,\varphi)=\sum_{nm}\psi_{nm}(r)\,S_{nm}(\theta,\varphi). \tag{15}$$

The deformation of the initial body can also be expressed as

$$\bar{u}(r,\theta,\varphi)=\begin{bmatrix} U_{nm}(r) \\ V_{nm}(r)\dfrac{\partial}{\partial\theta} \\ V_{nm}(r)\dfrac{1}{\sin\theta}\dfrac{\partial}{\partial\varphi}\end{bmatrix} S_{nm}(\theta,\varphi), \tag{16}$$

where r, θ, φ = spherical coordinate axis; r is the radial distance, θ is the co-latitude and φ is the east longitude, U_{nm} = radial dependence of the radial displacement, V_{nm} = radial dependence of the tangential displacement, and $S_{nm}(\theta,\varphi)$ = fully normalized spherical harmonic of degree n and order m. Equation (16) specifies a spheroidal motion which is appropriate for the deformation of the initial model.

Using Equations (14) through (16) we express Equations (12) and (13) in the following form, for the nth degree spherical harmonics.

$$\varrho_0\frac{\mathrm{d}}{\mathrm{d}r}\Psi_n+g_0\varrho_0x_n-g_0\Delta\varrho_n-\varrho_0\frac{\mathrm{d}}{\mathrm{d}r}(g_0U_n)+\frac{\mathrm{d}}{\mathrm{d}r}\left(\lambda x_n+2\mu\frac{\mathrm{d}}{\mathrm{d}r}U_n\right)+$$
$$+\frac{\mu}{r^2}\left[4r\frac{\mathrm{d}}{\mathrm{d}r}U_n-4U_n+n(n+1)\left(3V_n-U_n-r\frac{\mathrm{d}}{\mathrm{d}r}V_n\right)\right]=0 \tag{17}$$

$$\varrho_0\Psi_n-g_0\varrho_0U_n+\lambda x_n+r\frac{\mathrm{d}}{\mathrm{d}r}\left[\mu\left(\frac{\mathrm{d}}{\mathrm{d}r}V_n-\frac{V_n}{r}+\frac{U_n}{r}\right)\right]+$$
$$+\frac{\mu}{r}\left[5U_n+3r\frac{\mathrm{d}}{\mathrm{d}r}V_n-V_n-2n(n+1)V_n\right]=0 \tag{18}$$

and

$$\left[\frac{\mathrm{d}^2}{\mathrm{d}r^2}+\frac{2}{r}\frac{\mathrm{d}}{\mathrm{d}r}-\frac{n(n+1)}{r^2}\right]\Psi_n-4\pi G\left(\varrho_0x_n+U_n\frac{\mathrm{d}}{\mathrm{d}r}\varrho_0-\Delta\varrho_n\right)=0, \tag{19}$$

where g_0 = gravitational acceleration of the initial model, $g_0=-(\mathrm{d}/\mathrm{d}r)\Phi_G$, and X_n = radial dependence of the dilatation;

$$X_n(r)=\frac{\mathrm{d}}{\mathrm{d}r}U_n(r)-\frac{n(n+1)V_n(r)}{r}+2\frac{U_n(r)}{r}. \tag{20}$$

The subscript m is omitted in all of the variables because the equations turned out to be independent of the order of the harmonics. In deriving Equations (17) through (19) we made use of the following property of the spherical harmonics

$$\left[\frac{\partial^2}{\partial\theta^2} + \cot\theta\,\frac{\partial}{\partial\theta} + \frac{1}{\sin^2\theta}\,\frac{\partial^2}{\partial\varphi^2} + n(n+1)\right] S_{nm}(\theta, \varphi) = 0 .$$

Equations (17) through (19) differ from those of Alterman *et al.* (1959, Equations (23–25)) by an additional term in Equations (17) and (19) due to the density perturbations, $\Delta\varrho_n$, included in the present studies, and also by the lack of frequency terms in our equations since we are interested in the equations of the static deformation. These equations are three simultaneous second order ordinary differential equations. In order to simplify them we follow Alterman *et al.* (1959) and introduce the following dependent variables:

$$\bar{Y} = \begin{bmatrix} y_1 \\ y_2 \\ y_3 \\ y_4 \\ y_5 \\ y_6 \end{bmatrix} = \begin{bmatrix} U_n \\ \lambda x_n + 2\mu \dfrac{\mathrm{d}}{\mathrm{d}r} U_n \\ V_n \\ \mu\left(\dfrac{\mathrm{d}}{\mathrm{d}r} V_n - \dfrac{V_n}{r} + \dfrac{U_n}{r}\right) \\ \Psi_n \\ \dfrac{\mathrm{d}}{\mathrm{d}r} \Psi_n - 4\pi G\varrho_0 U_n \end{bmatrix}. \tag{21}$$

The components of vector $\bar{y}$ are physically meaningful; y_1 to y_5 denote the radial dependences of radial displacement, radial stress, tangential displacement, tangential stress, and gravitational perturbation, respectively. y_6 is the gradient of the gravitational potential minus the contribution of the radial displacement thereto. With this definition y_6 is continuous across the interface of two layers with different densities. Using Equation (21) we reduce Equations (17) through (19) into the following first order ordinary differential equation

$$\mathrm{d}\bar{Y}/\mathrm{d}r = \overline{\overline{M}} \cdot \bar{Y} + \bar{D}, \tag{22}$$

where

$$\overline{\overline{M}} = \begin{pmatrix} M_{11} & M_{12} & M_{13} & 0 & 0 & 0 \\ M_{21} & M_{22} & M_{23} & M_{24} & 0 & M_{26} \\ M_{31} & 0 & M_{33} & M_{34} & 0 & 0 \\ M_{41} & M_{42} & M_{43} & M_{44} & M_{45} & 0 \\ M_{51} & 0 & 0 & 0 & 0 & M_{56} \\ 0 & 0 & M_{63} & 0 & M_{65} & M_{66} \end{pmatrix},$$

with

$$M_{11} = -\,2\lambda/[r(\lambda + 2\mu)],$$
$$M_{12} = 1/(\lambda + 2\mu),$$

$$M_{13} = n(n+1)\,\lambda/[r(\lambda+2\mu)],$$
$$M_{21} = -\,4\varrho_0 g_0/r + 4\mu(3\lambda+2\mu)/[r^2(\lambda+2\mu)],$$
$$M_{22} = -\,4\mu/[r(\lambda+2\mu)],$$
$$M_{23} = n(n+1)\,[\varrho_0 g_0/r - 2\mu(3\lambda+2\mu)/(r^2(\lambda+2\mu))],$$
$$M_{24} = n(n+1)/r,$$
$$M_{26} = -\,\varrho_0,$$
$$M_{31} = -\,1/r,$$
$$M_{33} = 1/r,$$
$$M_{34} = 1/\mu,$$
$$M_{41} = \varrho_0 g_0/r - 2\mu(3\lambda+2\mu)/[r^2(\lambda+2\mu)],$$
$$M_{42} = -\,\lambda/[r(\lambda+2\mu)].$$
$$M_{43} = 2\mu[\lambda(2n^2+2n-1) + 2\mu(n^2+n-1)]/[r^2(\lambda+2\mu)].$$
$$M_{44} = -\,3/r,$$
$$M_{45} = -\,\varrho_0/r,$$
$$M_{51} = 4\pi G\varrho_0,$$
$$M_{56} = 1,$$
$$M_{63} = -\,4\pi G\varrho_0 n(n+1)/r,$$
$$M_{65} = n(n+1)/r^2,$$

and

$$M_{66} = -\,2/r,$$

and

$$\bar{D} = (0, g_0\Delta\varrho_n, 0, 0, 0, -\,4\pi G\Delta\varrho_n).$$

Notice that matrix $\bar{\bar{M}}$ depends on the physical properties of the initial model and the source vector $\bar{D}$ contains the density perturbations. In Paper I we started from this equation and developed the calculations. The general solution of Equation (22) is (Gantmacher, 1960)

$$\bar{Y}(r) = \bar{\bar{\Omega}}{}^r_\varepsilon(\bar{\bar{M}})\cdot\bar{Y}(\varepsilon) + \int\limits_\varepsilon^r \bar{\bar{\Omega}}{}^r_\tau(\bar{\bar{M}})\cdot\bar{D}_\tau\,\mathrm{d}\tau, \tag{23}$$

where $\bar{\bar{\Omega}}{}^r_\varepsilon(\bar{\bar{M}})$ and $\bar{\bar{\Omega}}{}^r_\tau(\bar{\bar{M}})$ are the matrizants of the media located between (ε, r) and (τ, r) respectively. $\bar{Y}(\varepsilon)$ is the value of $\bar{Y}$ near the center of the Moon, at $r=\varepsilon$. Since matrix $\bar{\bar{M}}$ is singular at the center, we have to start from a very small value of r, i.e. $r=\varepsilon$. Equation (23) contains six unknowns of $\bar{Y}(\varepsilon)$ plus an unknown function $\Delta\varrho_n$ which, in principle, introduces an infinite number of unknowns. These unknowns should be found from the boundary conditions imposed on the solution vector at the center and at the surface of the Moon.

B. BOUNDARY CONDITIONS

The boundary conditions appropriate to this problem are:

(1) Regularity of the solution at the center. This condition provides three independent parameters such that all of the components of $\bar{Y}(\varepsilon)$ can be expressed in terms of these parameters (paper 1).

(2) Vanishing of the stress on the deformed surface of the Moon. This surface is given by $r=a+U_a$ where a is the radius of the initial model and U_a is the radial displacement at the surface of this model. The radial stress, T_{rr}, at the deformed surface can be expressed by its Taylor series expansion about $r=a$ as

$$T_{rr}(r) = T_{rr}(a) + U_a \frac{\partial}{\partial r} T_{rr}(a) + \cdots .$$

Neglect of the terms with the higher powers of U_a reduces this expression into (Pekeris and Jarosch, 1958)

$$T_{rr}(r) = \lambda X(a) + 2\mu \frac{\mathrm{d}}{\mathrm{d}r} U_a .$$

Therefore, the vanishing of the radial stress at the deformed surface is equal to vanishing of y_2 at $r=a$, i.e.

$$y_2 = 0 . \tag{24}$$

If we follow the same procedure, the vanishing of the tangential stress at the deformed surface implies that, at $r=a$,

$$y_4 = 0 . \tag{25}$$

(3) Dirichlet's condition for the gravitational potential at $r=a$ implies that

$$y_5 = \delta\Phi_n , \tag{26}$$

where $\delta\Phi_n$ is the spherical harmonic coefficient of the observed gravitational potential; and

(4) Neumann's condition for the gravitational potential at $r=a$ leads to

$$\frac{\mathrm{d}}{\mathrm{d}r} y_5 - \frac{\partial}{\partial r} \delta\Phi_n = 4\pi G \varrho_0 U_a , \tag{27}$$

where $\varrho_0 U_a$ is regarded as a surface mass density at $r=a$. But the observed potential is the external potential and, therefore,

$$\frac{\partial}{\partial r} \delta\Phi_n + \frac{(n+1)}{r} \delta\Phi_n = 0 . \tag{28}$$

Taking into account Equations (21), (26) and (28), Equation (27) is reduced to

$$y_6 + \frac{(n+1)}{a} y_5 = 0 . \tag{29}$$

The boundary conditions at the surface can be put in the following compact form

$$\bar{\bar{B}}\cdot\bar{Y}(a)=\bar{b}, \tag{30}$$

where

$$\bar{\bar{B}}=\begin{bmatrix}0&1&0&0&0&0\\0&0&0&1&0&0\\0&0&0&0&1&0\\0&0&0&0&0&1\end{bmatrix}$$

and

$$\bar{b}=\begin{bmatrix}0\\0\\\delta\Phi_n\\-\dfrac{(n+1)}{a}\,\delta\Phi_n\end{bmatrix}.$$

These four boundary conditions are not enough to determine the above-mentioned three independent parameters together with the unknown density perturbations $\Delta\varrho_n$. Therefore, the problem is ill-posed. It would become well-posed if $\Delta\varrho_n$ is assumed to be a constant function. This is the case considered in Paper I. Such a case is a first order approximation and yields the overall effect of the actual density perturbations existing inside the Moon. In order to determine the density perturbations as functions of radius other constraints are needed. The constraint we adopt in the present paper is to make the total shear-strain energy of the Moon a minimum. Such a constraint reduces the strain tensor and the overall stress differences inside the Moon and therefore, it strengthens the stability of the present equilibrium state of the Moon. However, since the total volume of the Moon is considered in this constraint, the stress differences at some particular locations may not be reduced significantly.

C. SHEAR-STRAIN ENERGY

The total shear strain energy inside the Moon is defined by

$$\varepsilon_{\text{sh.}}=\int_v \mu\left[\sum_{ij}E_{ij}E_{ij}-\tfrac{1}{3}(\nabla\cdot\bar{u})^2\right]\mathrm{d}v, \tag{31}$$

where $E_{ij}=(i,j)$th element of the strain tensor and $v=$ the total volume of the Moon. Using the foregoing equations $\varepsilon_{\text{sh.}}$ is expressed in terms of y's as (Arkani-Hamed, 1969)

$$\varepsilon_{\text{sh.}}=\int_0^a \mu r^2\,\mathrm{d}r\,\bar{Y}'^{T}\cdot\bar{\bar{P}}\cdot\bar{Y}', \tag{32}$$

where

$$\bar{Y}'=\begin{bmatrix}y_1\\y_2\\y_3\\y_4\end{bmatrix}=\bar{\bar{\beta}}\cdot\bar{Y},$$

with

$$\bar{\bar{\beta}} = \begin{bmatrix} 1 & 0 & 0 & 0 & 0 & 0 \\ 0 & 1 & 0 & 0 & 0 & 0 \\ 0 & 0 & 1 & 0 & 0 & 0 \\ 0 & 0 & 0 & 1 & 0 & 0 \end{bmatrix},$$

and

$$\bar{\bar{P}} = \begin{pmatrix} P_{11} & P_{12} & P_{13} & & \\ P_{12} & P_{22} & P_{23} & 0 & \\ P_{13} & P_{23} & P_{33} & & \\ & 0 & & P_{44} & \\ & & & 0 & \end{pmatrix}$$

with

$$\begin{aligned} P_{11} &= 2(3\lambda + 2\mu)^2/[3r^2(\lambda + 2\mu)^2], \\ P_{12} &= -2(3\lambda + 2\mu)/[3r(\lambda + 2\mu)^2], \\ P_{13} &= -n(n+1)P_{11}/2, \\ P_{22} &= 2/[3(\lambda + 2\mu)^2], \\ P_{23} &= -n(n+1)P_{12}/2, \\ P_{33} &= 2n^2(n+1)^2(3\lambda^2 + 4\mu^2 + 6\mu\lambda)/[r^2(\lambda + 2\mu)^2] - n(n+1)/r^2, \end{aligned}$$

and

$$P_{44} = n(n+1)/2\mu^2.$$

D. DETERMINATION OF DENSITY PERTURBATIONS

It was mentioned before that the density perturbations introduce an infinite number of unknowns. In practice, however, we consider some finite number of these unknowns. For example, we express the density perturbations in terms of a polynomial or any regular function of r with finite terms or we stratify the lunar interior into finite number of layers and assume that the density perturbations within each layer does not change with depth. In these cases the density perturbations are regarded as components of a finite dimensional vector and, therefore, the source vector can be written as

$$\bar{D} = \bar{\bar{H}} \cdot \bar{X}, \tag{33}$$

where $\bar{\bar{H}}$ = a known matrix which depends on the geometry and the physical properties of the initial model and $\bar{X}$ = the unknown vector wich in the case of polynomial expansion contains the coefficients of the terms and in the case of a layered model contains the density perturbation of each layer. Substituting Equation (33) into (23) yields

$$\bar{Y}(r) = \Omega_\varepsilon^r(\bar{\bar{M}}) \cdot \bar{Y}(\varepsilon) + \bar{\bar{\Gamma}} \cdot \bar{X}, \tag{34}$$

where $\bar{\bar{\Gamma}}$ is a known source propagator whose exact expression is presented in an appendix. On the other hand, the condition at the center of the Moon provides the value of $\bar{Y}(\varepsilon)$ as

$$\bar{Y}(\varepsilon) = \bar{\bar{C}} \cdot \bar{\alpha}, \tag{35}$$

where $\bar{\bar{C}}$ is also a known matrix (pare 1) and $\bar{\alpha}$ is the unknown vector which contains the three independent parameters near the center. Therefore Equation (34) can be written as

$$\bar{Y}(r) = \bar{\bar{Q}}(r)\cdot\bar{\xi}, \tag{36}$$

where

$$\bar{\bar{Q}}(r) = [\Omega_\varepsilon^r(\bar{\bar{M}})\cdot\bar{\bar{C}} \,\vdots\, \bar{\bar{\Gamma}}],$$

and

$$\bar{\xi} = \begin{bmatrix} \bar{\alpha} \\ \cdots \\ \bar{X} \end{bmatrix}.$$

Using expression (36) the boundary condition at the surface, Equation (30), becomes

$$\bar{\bar{\varkappa}}\cdot\bar{\xi} = \bar{b}, \tag{37}$$

where

$$\bar{\bar{\varkappa}} = \bar{\bar{B}}\cdot\bar{\bar{Q}}(\alpha),$$

and the total shear strain energy, Equation (32), becomes

$$\varepsilon_{\text{sh.}} = \bar{\xi}^T\cdot\bar{\bar{W}}\cdot\bar{\xi}, \tag{38}$$

where

$$\bar{\bar{W}} = \int_0^a \mu r^2 \,\mathrm{d}r \bar{\bar{Q}}^T\cdot\bar{\bar{\beta}}^T\cdot\bar{\bar{P}}\cdot\bar{\bar{\beta}}\cdot\bar{\bar{Q}}.$$

Now the determination of the density perturbations is reduced to the determination of the unknown vector $\bar{\xi}$ such that it satisfies Equation (37) and also minimizes the shear strain energy. This is a generalized least squares problem and can be solved by introducing Lagrangian multipliers which leads to the following first order simultaneous linear equations,

$$\bar{\bar{V}}\cdot\bar{z} = \bar{d}, \tag{39}$$

where

$$\bar{\bar{V}} = \begin{bmatrix} \bar{\bar{W}} & \bar{\bar{\varkappa}}^T \\ \bar{\bar{\varkappa}} & 0 \end{bmatrix},$$

with

$$\bar{z} = \begin{bmatrix} \bar{\xi} \\ \cdots \\ \bar{\Lambda} \end{bmatrix},$$

where $\bar{\Lambda}$ = Lagrangian multipliers, and

$$\bar{d} = \begin{bmatrix} 0 \\ \cdots \\ \bar{b} \end{bmatrix}.$$

The solution of Equation (39) is

$$\bar{\xi} = (\bar{\bar{W}}^{-1}\,\bar{\bar{\varkappa}}\cdot{}^T)\cdot(\bar{\bar{\varkappa}}\cdot\bar{\bar{W}}^{-1}\cdot\bar{\bar{\varkappa}}^T)^{-1}\cdot\bar{b} \tag{40}$$

This is the formula through which we determine the density perturbations to be presented in the next sections. The numerical procedure is similar to the one presented in Paper I and will not be described in the present paper.

3. Lateral Variations of Density in the Moon

In this section a general behavior of the solution vector ξ is investigated and a criterion is found for selecting a geophysically plausible lunar density model. Using the criterion we then present a model for the lateral variations of density inside the Moon. The variations are determined for a layered initial lunar model whose physical properties are given in Table III. It is assumed that the density perturbations of a layer are

TABLE III

Initial model of the Moon

r (km)	g (cm s^{-2})	ϱ (g cc^{-1})	λ ($\times 10^{11}$ dyn cm^{-2})	μ
		3.374	6	4
300	28.2801			
		3.374	6	4
500	47.1335			
		3.374	6	4
700	65.9869			
		3.374	6	4
900	84.8403			
		3.374	6	4
1100	103.6937			
		3.374	6	4
1200	113.1204			
		3.374	6	4
1300	122.5470			
		3.374	6	4
1400	131.9737			
		3.374	6	4
1500	141.4004			
		3.374	6	4
1600	150.8271			
		3.374	6	4
1685	158.8398			
		3.2	4	3
1735	162.8709			

independent of the depth within the layer. It was pointed out in Paper I that the effects of the lateral variations of density within the surface layer do not penetrate deeper than about 800 km if the variations are specified by the spherical harmonics with degrees higher than 6. This implies that any plausible higher harmonics of the lateral variations of density probably existing deeper than about 800 km cannot be resolved from the observations of the gravitational potential at the lunar surface. Therefore we divide the density perturbations into two groups; those characterized by the spherical harmonics of degrees lower than 7, and those specified by the higher harmonics. The first group is assumed to be distributed throughout the Moon (excluding the central sphere of radius $r=\varepsilon=300$ km) while the second group is confined to the region above 1300 km radius. This is the region where the resolving power of the observed gravitational potential is good (Paper I).

A. PRELIMINARY INVESTIGATION

The assumption that the lunar model is a linearly elastic body makes the superposition theorem valid for the response of the model to the density perturbations and allows us to study each harmonic of the density perturbations separately. Furthermore, since the boundary condition explained in the previous section, Equation (30), contains only the gravitational potential data we can determine the density perturbations

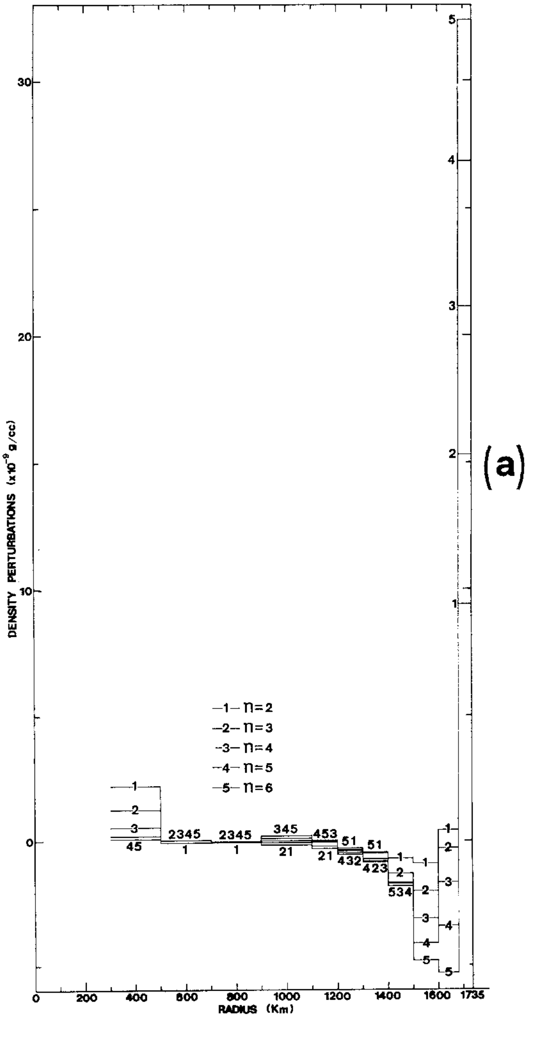

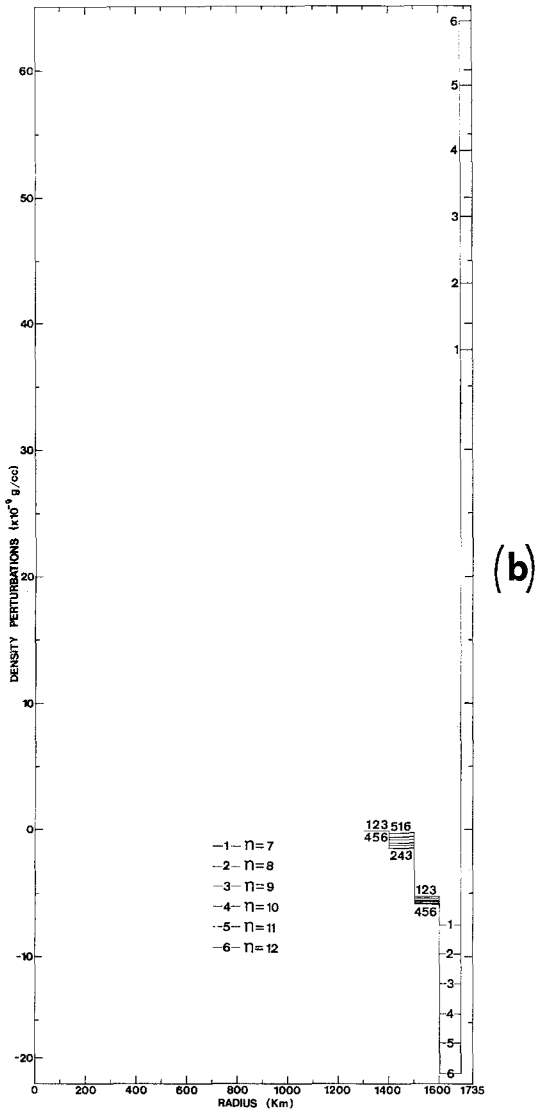

Fig. 5. Radial variations of density perturbations when only the shear strain energy is minimized: (a) for harmonic with degrees less than 7; (b) for higher degree harmonics.

in the normalized sense; a density perturbation such that the gravitational potential at the deformed surface of the Moon be specified by a spherical harmonic of degree n and with an amplitude of 1 erg. This is the procedure we follow in this preliminary investigation. Figure 5 illustrates the radial dependence of the density perturbations determined through Equation (40). The perturbations oscillate strongly with depth. Such an oscillatory behavior of the solution of Equation (40) has already been noted in the determination of the density perturbations inside the earth (Kaula, 1963; Arkani-Hamed, 1970). The radial oscillations of the density perturbations inside the

Moon are difficult to explain geophysically. In order to avoid this behavior we introduce another constraint for the determination of the solution vector $\bar{\xi}$; we also minimize the mass perturbations of each layer, γ_i, along with the minimization of the shear-strain energy, where

$$\gamma_i = h_i \Delta \varrho_{n,i}\,; \tag{41}$$

h_i being the thickness of the ith layer. The minimization of the mass perturbations is accomplished by the minimization of the length of vector $\bar{\gamma}$ whose ith component is defined by Equation (41). We express the square of the length of $\bar{\gamma}$ in terms of $\bar{\xi}$ as

$$|\gamma|^2 = \bar{\xi}^T \cdot \overline{\overline{W}}_m \cdot \bar{\xi}\,, \tag{42}$$

where

$$\overline{\overline{W}}_m = \begin{bmatrix} 0 & & & & & & & & & \\ & 0 & & & & & & & & \\ & & 0 & & & 0 & & & & \\ & & & h_1^2 & & & & & & \\ & & & & h_2^2 & & & & & \\ & & & & & \cdot & & & & \\ & & & & & & \cdot & & & \\ & & & & & & & \cdot & & \\ & & 0 & & & & & h_i^2 & & \\ & & & & & & & & \cdot & \\ & & & & & & & & & \cdot \\ & & & & & & & & & & \cdot \end{bmatrix}.$$

Now we determine $\bar{\xi}$ in such a way that it satisfies Equation (37) and also it minimizes expressions (38) and (42). The final formula for $\bar{\xi}$ is similar to Equation (40) where $\overline{\overline{W}}$ is to be replaced by $\overline{\overline{W}} + \omega_m \overline{\overline{W}}_m$. ω_m is a weighting factor which emphasizes the relative strength of the minimization of $\overline{\overline{W}}$ and $\overline{\overline{W}}_m$. We determine the density perturbations by the new formula for different values of the weighting factor ω_m. Figure 6 illustrates the perturbations thus determined for the 2nd and the 12th degree harmonics. The behavior of the density perturbations of the other harmonics are similar to these figures. It is clear from the figures that the oscillatory behavior of the density perturbations vanishes gradually as the value of ω_m increases. In general, the amplitude of the density perturbations decreases with depth (this is especially evident for the non-oscillatory perturbations) which indicates that the upper 300 km of the lunar interior is mostly responsible for the observed gravitational undulations. Figure 7 shows the total shear strain energy as a function of ω_m for different harmonics. The strong variation of the energy occurs when ω_m is between 10^{-5} and 10^{-1}. This is the region where $\overline{\overline{W}}$ and $\overline{\overline{W}}_m$ are comparable. When $\omega_m < 10^{-5}$ $\overline{\overline{W}}$ is the dominant element, thus the energy obtains values very close to its minimum value, and when $\omega_m > 10^{-1}$ $\overline{\overline{W}}_m$ is the dominant element, therefore the energy obtains values very far from its minimum value. The oscillatory behavior of the perturbations just disappears at the ω_m value of about 5×10^{-3}. The corresponding energy is closer to its upper limiting value. The

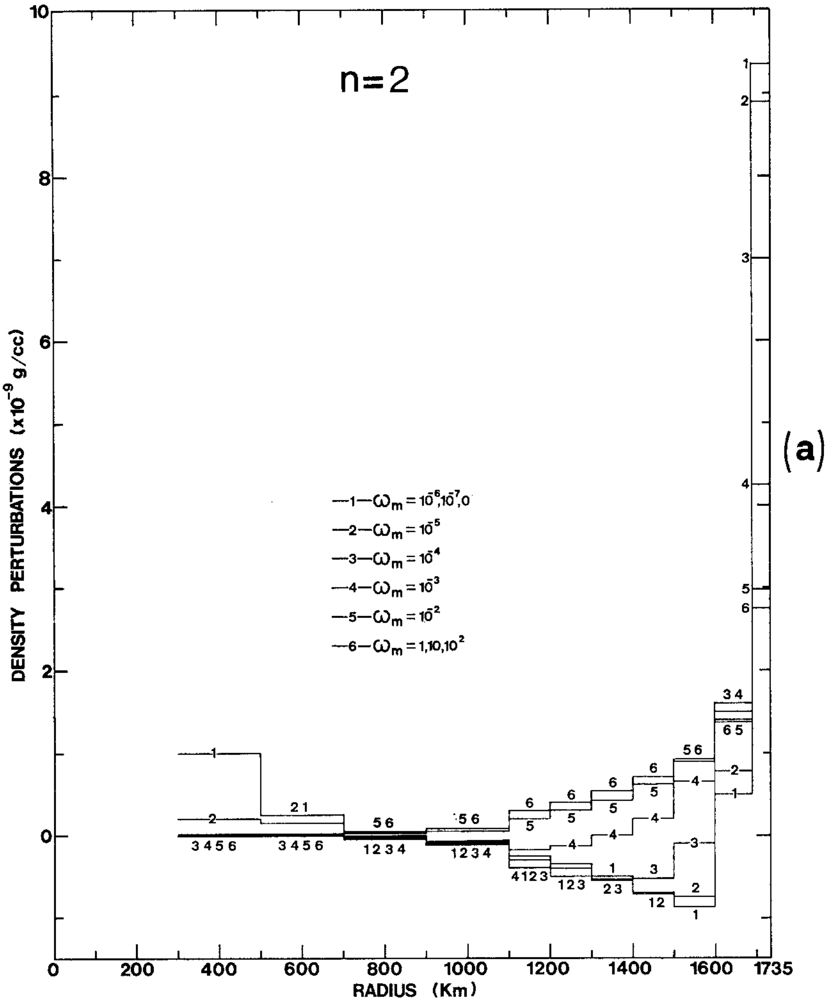

two limiting values of the energy, however, differ from each other by a factor of about 2, which implies that the shear stresses may change by a factor of about $\sqrt{2}$ for the two limiting cases. When ω_m equals to 10^{-3}, however, the oscillations are very small but the corresponding energy is about the average of the upper and lower limiting values. We select the ω_m value of 10^{-3} in the determination of the density perturbations to be presented in the following section.

B. DENSITY MODEL

The lateral variations of density in the Moon are determined through Equation (40) where $\overline{\overline{W}}$ is replaced by $\overline{\overline{W}}+\omega_m\overline{\overline{W}}_m$. It is required that the gravitational potential at the surface of the Moon, after being deformed under the influence of the density perturbations, to be equal to the observed lunar gravitational potential presented by Michael and Blackshear (1971), whose spherical harmonic coefficients are given in

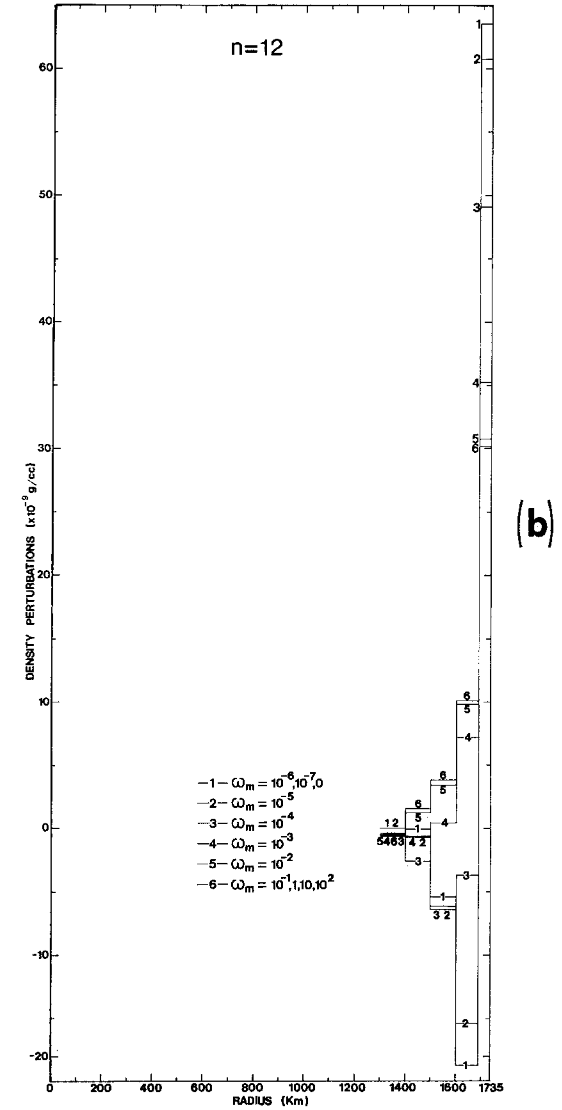

Fig. 6. Effects of the weighting factor, ω_m, on the radial variations of the density perturbations: (a) for the second degree harmonics; (b) for the 12th degree harmonics.

Table II. From all possible density perturbations we select the one which corresponds to ω_m value of 10^{-3}. Table IV shows the spherical harmonic coefficients of the selected perturbations for each layer. Figure 8 displays the lateral variations of density within 0–50 km of the surface. The variations are within ± 0.2 g cc^{-1} except at the polar regions and the regions close to the limb where the density perturbations thus found are probably not meaningful since the input gravitational expression is not reliable in these regions (Michael and Blackshear, 1971). In general, the filled circular mare

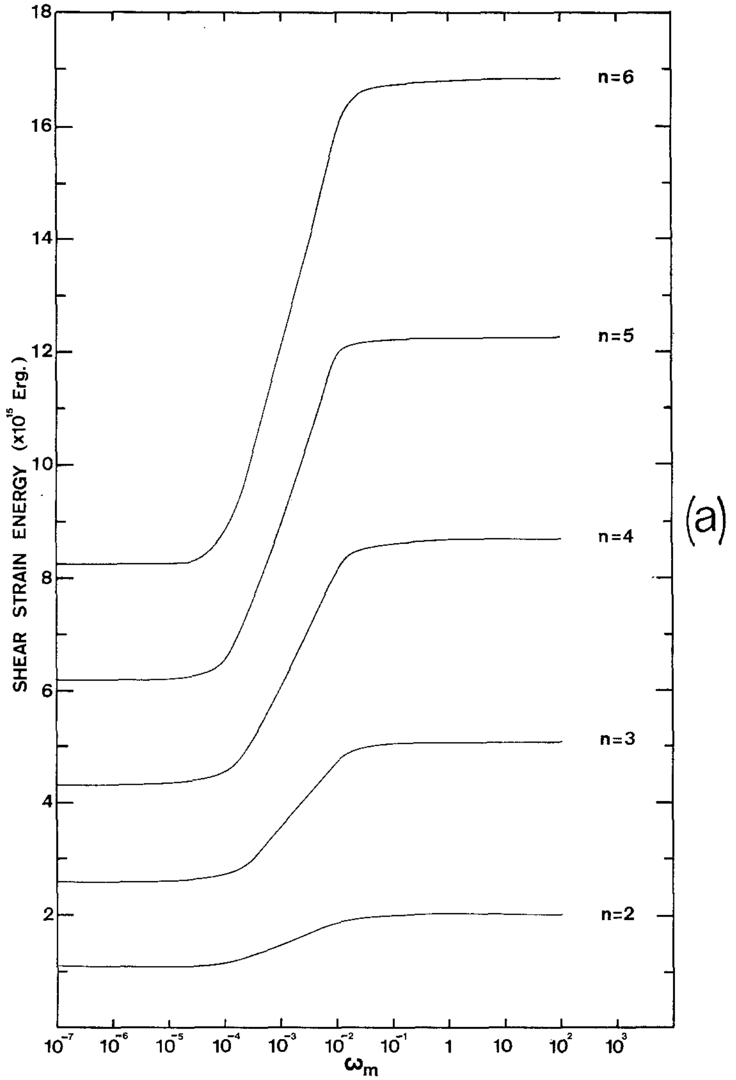

areas are associated with positive density anomalies while the highlands have negative density anomalies. Maria Procellarum and Tranquillitatis have negligible anomalies in comparison to the anomalies associated with maria Serenitatis, Imbrium, Crisium, and Nectaris. Figure 9 illustrates the radial variations of the density perturbations under some mare regions. The density anomalies decreases rapidly with depth and becomes negligible below 300 km where they exhibit oscillatory behavior. This implies that the density perturbations of the upper 300 km of the lunar interior are responsible for the undulations of the gravitational potential of the Moon.

Figure 10 illustrates the lateral undulations of the gravitational potential at the surface of the Moon which arise from the presence of the density perturbations and also from the deformation of the Moon. The potential is equal to Michael and Black-

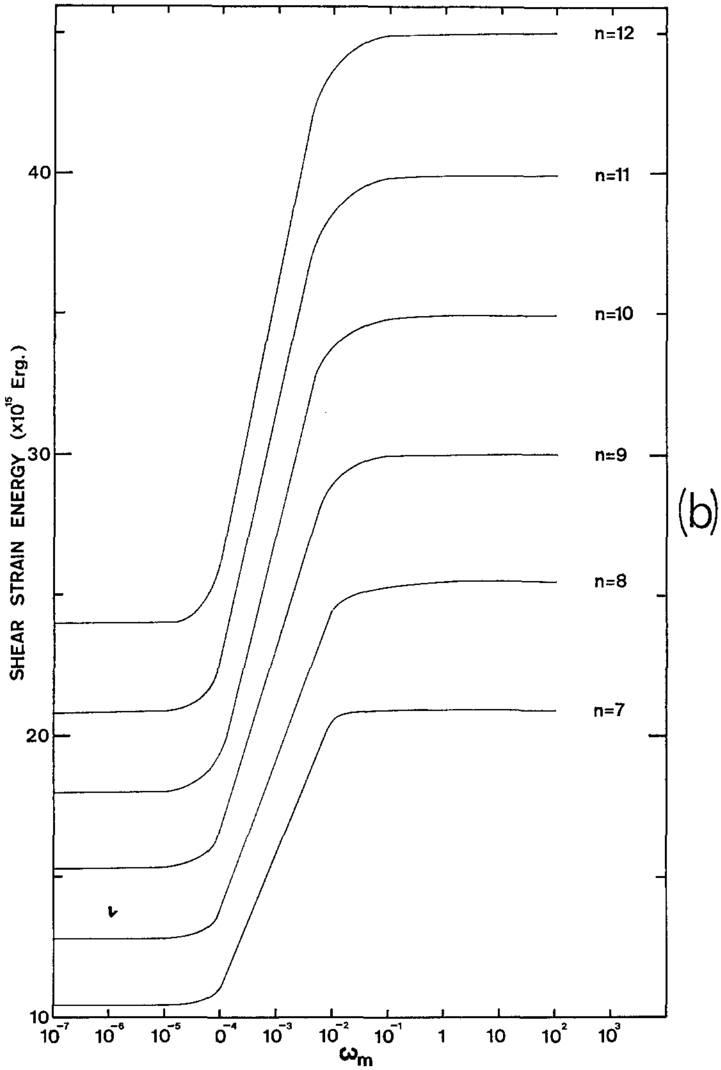

Fig. 7. Total shear-strain energy of the deformation of the Moon as functions of the weighting factor, ω_m: (a) for the second to 6th degree harmonics; (b) for the 7th to 12th degree harmonics.

shear's (1971) presentation where harmonics through the 12th degree are used. The radial variations of the potential are shown under some mare regions (Figure 11). The potential achieves maximum values at the bottom of the first layer, 50 km deep, and then decreases with increasing depth. Below 900 km the undulations become negligible. Figure 12 displays the lateral variations of the radial displacement at the surface of the Moon. In general, mare regions are depressed while highland areas are raised. The topography thus created at the surface of the Moon is within ± 60 meters which is negligible compared with the measured topography (Wollenhaupt and Sjo-

TABLE IV

Fully normalized spherical harmonic coefficients of the density perturbations. (1) = layer between 0–50 km depths, (2) = layer between 50–135 km depths, ..., and (11) = layer between 1235–1435 km depths. Units are in g cc^{-1}

n	m	Odd	Even	n	m	Odd	Even
			(1)				
2	0	.00000000	.00000000	9	2	−.31906038 − 002	−.44456404 − 002
2	1	.12140674 − 002	.10315522 − 002	9	3	−.50620631 − 002	−.11901889 − 001
2	2	−.19496720 − 005	.46396394 − 002	9	4	.17294355 − 001	−.68053065 − 002
3	0	.00000000	.20851002 − 002	9	5	−.17114359 − 001	.59447804 − 002
3	1	.37357473 − 002	.43369809 − 002	9	6	.66055855 − 002	−.27171912 − 001
3	2	.12896324 − 002	.43335492 − 002	9	7	.29514318 − 001	−.29489661 − 001
3	3	−.43294321 − 003	.19629317 − 002	9	8	.56883486 − 001	−.26974657 − 002
4	0	.00000000	.31224715 − 002	9	9	−.49165874 − 002	.16103426 − 001
4	1	−.24228544 − 002	−.56628845 − 002	10	0	.00000000	−.33787323 − 002
4	2	−.50311264 − 002	−.30727719 − 002	10	1	.57873058 − 003	.45704014 − 001
4	3	−.12510913 − 002	−.25451918 − 002	10	2	.76182702 − 002	.65555818 − 004
4	4	.14584914 − 002	−.69005951 − 003	10	3	−.49517355 − 002	−.30394571 − 003
5	0	.00000000	−.28019761 − 002	10	4	.15160834 − 001	.52657753 − 002
5	1	−.37730313 − 002	−.30552411 − 002	10	5	−.27195290 − 001	.48620098 − 002
5	2	.83614524 − 003	.74645235 − 003	10	6	.17866624 − 001	−.52797949 − 002
5	3	.93819251 − 002	.42313792 − 002	10	7	−.14628088 − 001	.25995209 − 001
5	4	−.66330730 − 002	.42116122 − 002	10	8	−.28019645 − 001	.37965175 − 001
5	5	−.29774084 − 002	.26611360 − 002	10	9	−.15410384 − 001	.39395177 − 002
6	0	.00000000	.59389966 − 002	10	10	.63200519 − 002	−.14344892 − 001
6	1	−.52418167 − 002	−.10160215 − 001	11	0	.00000000	.94878062 − 002
6	2	.62852982 − 003	−.19084728 − 002	11	1	.43005919 − 001	−.11674387 − 001
6	3	−.24622503 − 002	.24286880 − 002	11	2	.12485284 − 001	−.55563774 − 002
6	4	−.11049615 − 001	−.38672891 − 002	11	3	.10819317 − 001	.45151482 − 002
6	5	.43386864 − 002	−.51731666 − 002	11	4	.27964891 − 001	.21783776 − 002
6	6	.55026870 − 002	−.75469345 − 002	11	5	−.19855924 − 001	−.71424630 − 002
7	0	.00000000	−.97036850 − 002	11	6	.28422400 − 001	.14154406 − 001
7	1	−.20046973 − 001	.29494817 − 002	11	7	−.34770743 − 001	−.29949537 − 002
7	2	−.38449253 − 002	−.43237135 − 002	11	8	.53355106 − 002	−.18120542 − 001
7	3	−.64197826 − 002	−.46690989 − 002	11	9	.37231830 − 001	−.41365194 − 001
7	4	−.61785610 − 003	−.10136787 − 001	11	10	.19231187 − 001	−.13977712 − 001
7	5	.15918795 − 001	.27228796 − 002	11	11	−.52282324 − 002	.32151894 − 002
7	6	−.52849448 − 002	.34410619 − 002	12	0	.00000000	.19418080 − 002
7	7	−.34520266 − 002	.95574901 − 002	12	1	.25366341 − 002	.22448526 − 001
8	0	.00000000	−.25533735 − 002	12	2	.11674782 − 001	−.33584796 − 002
8	1	.32318474 − 002	.12058429 − 001	12	3	.23462194 − 002	.14420133 − 002
8	2	.67290916 − 002	.30049760 − 002	12	4	.40828300 − 002	.12843316 − 001
8	3	−.11581143 − 001	.56182778 − 003	12	5	−.18077082 − 001	.35513581 − 002
8	4	.11611108 − 001	−.29899940 − 002	12	6	.25222034 − 002	.71695902 − 002
8	5	−.30649043 − 002	.15044143 − 001	12	7	−.24933420 − 001	−.32363467 − 002
8	6	−.22580126 − 001	.78891322 002	12	8	.43679241 − 001	.55610960 − 002
8	7	.25533735 − 002	−.17623200 − 002	12	9	−.10002933 − 001	−.15303573 − 001
8	8	.56632241 − 002	−.17085986 − 001	12	10	−.35407991 − 001	.33116679 − 001
9	0	.00000000	−.10392887 − 001	12	11	−.96967212 − 002	.11766294 − 001
9	1	−.56045151 − 002	.57647850 − 003	12	12	.50472226 − 003	−.26429285 − 003
			(2)				
2	0	.00000000	.00000000	9	2	−.74024420 − 003	−.10314222 − 002
2	1	.45897999 − 003	.38997983 − 003	9	3	−.11744369 − 002	−.27613282 − 002

Table IV (Continued)

n	*m*	Odd	Even	*n*	*m*	Odd	Even
2	2	−.73707639 − 006	.17540226 − 002	9	4	.40124210 − 002	−.15788825 − 002
3	0	.00000000	.70880977 − 003	9	5	−.39706607 − 002	.13792340 − 002
3	1	.12699314 − 002	.14743150 − 002	9	6	.15325458 − 002	−.63040889 − 002
3	2	.43839814 − 003	.14731484 − 002	9	7	.68475449 − 002	−.68418243 − 002
3	3	−.14717485 − 003	.66727977 − 003	9	8	.13197399 − 001	−.62583242 − 003
4	0	.00000000	.97434348 − 003	9	9	−.11406854 − 002	.37361166 − 002
4	1	−.75603328 − 003	−.17670600 − 002	10	0	.00000000	−.75021959 − 003
4	2	−.15699247 − 002	−.95883511 − 003	10	1	.12850234 − 003	.10148199 − 001
4	3	−.39039352 − 003	−.79420774 − 003	10	2	.16915740 − 002	.14556128 − 004
4	4	.45511116 − 003	−.21532782 − 003	10	3	−.10994919 − 002	−.67488634 − 004
5	0	.00000000	−.81251388 − 003	10	4	.33663380 − 002	.11692219 − 002
5	1	−.10940994 − 002	−.88595539 − 003	10	5	−.60384895 − 002	.10795691 − 002
5	2	.24246446 − 003	.21645542 − 003	10	6	.39671363 − 002	−.11723348 − 002
5	3	.27205601 − 002	.12270106 − 002	10	7	−.32480461 − 002	.57720214 − 002
5	4	−.19234511 − 002	.12212786 − 002	10	8	−.62215306 − 002	.84298533 − 002
5	5	−.86338556 − 003	.77167324 − 003	10	9	−.34217484 − 002	.87473737 − 003
6	0	.00000000	.16149695 − 002	10	10	.14033153 − 002	−.31851647 − 002
6	1	−.14253879 − 002	−.27628299 − 002	11	0	.00000000	.20211106 − 002
6	2	.17091380 − 003	−.51896400 − 003	11	1	.91612031 − 002	−.24869003 − 002
6	3	−.66955068 − 003	.66042421 003	11	2	.26596391 002	−.11836301 − 002
6	4	−.30046813 − 002	−.10516177 − 002	11	3	.23047517 002	.96182550 − 003
6	5	.11798030 − 002	−.14067202 − 002	11	4	.59571345 − 002	.46404216 − 003
6	6	.14963255 − 002	−.20522102 − 002	11	5	−.42297470 − 002	−.15217141 − 002
7	0	.00000000	−.24818877 − 002	11	6	.60545941 − 002	.30151986 − 002
7	1	−.51273649 − 002	.75438167 − 003	11	7	−.74069302 − 002	−.63799075 − 003
7	2	−.98340709 − 003	−.11058656 − 002	11	8	.11365807 − 002	−.28600726 − 002
7	3	−.16419720 − 002	−.11942039 − 002	11	9	.79311956 − 002	−.88116928 − 002
7	4	−.15802754 − 003	−.25926612 − 002	11	10	.40966642 − 002	−.29775590 − 002
7	5	.40715110 − 002	.69642422 − 003	11	11	−.11137281 − 002	.68490579 − 003
7	6	−.13517173 − 002	.88011195 − 003	12	0	.00000000	.39764288 − 003
7	7	−.88291634 − 003	.24444958 − 002	12	1	.51945120 − 003	.45970025 − 002
8	0	.00000000	−.62088348 − 003	12	2	.23907585 − 002	−.68774848 − 003
8	1	.78586258 − 003	.29321522 − 002	12	3	.48045812 − 003	.29529507 − 003
8	2	.16362596 − 002	.73069607 − 003	12	4	.83608074 − 003	.26300505 − 002
8	3	−.28160943 − 002	.13661518 − 003	12	5	−.37018195 − 002	.72724609 − 003
8	4	.28233805 − 002	−.72705299 − 003	12	6	.51649608 − 003	.14681866 − 002
8	5	−.74526835 − 003	.36581643 − 002	12	7	−.51058586 − 002	−.66273814 − 003
8	6	−.54906293 − 002	.19183374 − 002	12	8	.89446224 − 002	.11387996 − 002
8	7	.62088348 − 003	−.42852930 − 003	12	9	−.20483978 − 002	−.31338612 − 002
8	8	.13770810 − 002	−.41546629 − 002	12	10	−.72508381 − 002	.67816238 − 002
9	0	.00000000	−.24112282 − 002	12	11	−.19856917 − 002	.24094982 − 002
9	1	−.13002899 − 002	.13374737 − 003	12	12	.10335688 − 003	−.54121813 − 004

(3)

2	0	.00000000	.00000000	9	2	−.61680859 − 004	−.85943267 − 004
2	1	.18815735 − 003	.15987096 − 003	9	3	−.97859971 − 004	−.23008772 − 003
2	2	−.30216206 − 006	.71905583 − 003	9	4	.33433504 − 003	−.13156041 − 003
3	0	.00000000	.22223871 − 003	9	5	−.33085536 − 003	.11492469 − 003
3	1	.39817160 − 003	.46225360 − 003	9	6	.12769940 − 003	−.52528830 − 003
3	2	.13745442 − 003	.46188783 − 003	9	7	.57057178 − 003	−.57009411 − 003
3	3	−.46144891 − 004	.20921748 − 003	9	8	.10996734 − 002	−.52147496 − 004
4	0	.00000000	.23810487 − 003	9	9	−.95047629 − 004	.31131197 − 003
4	1	−.18475539 − 003	−.43182473 − 003	10	0	.00000000	−.54485076 − 004
4	2	−.38364985 − 003	−.23431502 − 003	10	1	.93325474 − 005	.73701804 − 003

Table IV (Continued)

n	m	Odd	Even	n	m	Odd	Even
4	3	−.95402289 − 004	−.19408426 − 003	10	2	.12285141 − 003	.10571461 − 005
4	4	.11121764 − 003	−.52620667 − 004	10	3	−.79851157 − 004	−.49013960 − 005
5	0	.00000000	−.15624529 − 003	10	4	.24448200 − 003	.84915330 − 004
5	1	−.21039378 − 003	−.17036799 − 003	10	5	−.43854834 − 003	.78404250 − 004
5	2	.46625577 − 004	.41624075 − 004	10	6	.28811527 − 003	−.85141409 − 004
5	3	.52315992 − 003	.23595243 − 003	10	7	−.23589099 − 003	.41919597 − 003
5	4	−.36987696 − 003	.23485017 − 003	10	8	−.45184180 − 003	.61222235 − 003
5	5	−.16602784 − 003	.14839169 − 003	10	9	−.24850621 − 003	.63528242 − 004
6	0	.00000000	.24739070 − 003	10	10	.10191648 − 003	−.23132419 − 003
6	1	−.21834946 − 003	−.42322683 − 003	11	0	.00000000	.13099499 − 003
6	2	.26181600 − 004	−.79498012 − 004	11	1	.59376842 − 003	−.16118439 − 003
6	3	−.10256578 − 003	.10116773 − 003	11	2	.17238017 − 003	−.76715055 − 004
6	4	−.46027506 − 003	−.16109309 − 003	11	3	.14937872 − 003	.62339150 − 004
6	5	.18072929 − 003	−.21548982 − 003	11	4	.38610195 − 003	.30076135 − 004
6	6	.22921609 − 003	−.31436984 − 003	11	5	−.27414414 − 003	−.98627418 − 004
7	0	.00000000	−.29118914 − 003	11	6	.39241863 − 003	.19542518 − 003
7	1	−.60157154 − 003	.88508338 − 004	11	7	−.48006809 − 003	−.41350329 − 004
7	2	−.11537890 − 003	−.12974642 − 003	11	8	.73665620 − 004	−.25018430 − 003
7	3	−.19264547 − 003	−.14011078 − 003	11	9	.51404750 − 003	−.57111548 − 003
7	4	−.18540687 − 004	−.30418572 − 003	11	10	.26551860 − 003	−.19298563 − 003
7	5	.47769277 − 003	.81708441 − 004	11	11	−.72184467 − 004	.44391051 − 004
7	6	−.15859115 − 003	.10325973 − 003	12	0	.00000000	.23545492 − 004
7	7	−.10358876 − 003	.28680211 − 003	12	1	.30758086 − 004	.27220074 − 003
8	0	.00000000	−.60717005 − 004	12	2	.14156316 − 003	−.40723416 − 004
8	1	.76850526 − 004	.28673898 − 003	12	3	.28449203 − 004	.17485206 − 004
8	2	.16001196 − 003	.71455721 − 004	12	4	.49506563 − 004	.15573228 − 003
8	3	−.27538954 − 003	.13359777 − 004	12	5	−.21919458 − 003	.43062175 − 004
8	4	.27610206 − 003	−.71099460 − 004	12	6	.30583106 − 004	.86935232 − 004
8	5	−.72880764 − 004	.35773666 − 003	12	7	−.30233146 − 003	−.39242487 − 004
8	6	−.53693580 − 003	.18759672 − 003	12	8	.52963487 − 003	.67431354 − 004
8	7	.60717005 − 004	−.41906439 − 004	12	9	−.12129108 − 003	−.18556426 − 003
8	8	.13466655 − 003	−.40628990 − 003	12	10	−.42934140 − 003	.40155798 − 003
9	0	.00000000	−.20091563 − 003	12	11	−.11757809 − 003	.14267279 − 003
9	1	−.10834667 − 003	.11144501 − 004	12	12	.61200355 − 005	−.32046964 − 003

(4)

2	0	.00000000	.00000000	9	2	.93808293 − 004	.13070815 − 003
2	1	.60642209 − 004	.51525642 − 004	9	3	.14883186 − 003	.34993248 − 003
2	2	−.97385381 − 007	.23174824 − 003	9	4	−.50847864 − 003	.20008569 − 003
3	0	.00000000	.10230919 − 004	9	5	.50318652 − 003	−.17478500 − 003
3	1	.18330116 − 004	.21280177 − 004	9	6	−.19421361 − 003	.79889288 − 003
3	2	.63278133 − 005	.21263338 − 004	9	7	−.86776296 − 003	.86703801 − 003
3	3	−.21243133 − 005	.96314774 − 005	9	8	−.16724554 − 002	.79309329 − 004
4	0	.00000000	−.52686650 − 004	9	9	.14455466 − 003	−.47346365 − 003
4	1	.40881744 − 004	.95552006 − 004	10	0	.00000000	.87975976 − 004
4	2	.84892111 − 004	.51848050 − 004	10	1	−.15069080 − 004	−.11900485 − 002
4	3	.21110139 − 004	.42945990 − 004	10	2	−.19836575 − 003	−.17069530 − 005
4	4	−.24609681 − 004	.11643637 − 004	10	3	.12893409 − 003	.79141874 − 005
5	0	.00000000	.76917960 − 004	10	4	−.39476025 − 003	−.13711111 − 003
5	1	.10357471 − 003	.83870421 − 004	10	5	.70811534 − 003	−.12659779 − 003
5	2	−.22953296 − 004	−.20491107 − 004	10	6	−.46521404 − 003	.13747615 − 003
5	3	−.25754629 − 003	−.11615697 − 003	10	7	.38088852 − 003	−.67686744 − 003
5	4	.18208665 − 003	−.11561434 − 003	10	8	.72958002 − 003	−.98854333 − 003
5	5	.81733811 − 004	−.73051714 − 004	10	9	.40125806 − 003	−.10257780 − 003

Table IV (Continued)

n	m	Odd	Even	n	m	Odd	Even
6	0	.00000000	−.18813051 − 003	10	10	−.16456253 − 003	.37351460 − 003
6	1	.16604583 − 003	.32184670 − 003	11	0	.00000000	−.21585851 − 003
6	2	−.19910036 − 004	.60454988 − 004	11	1	−.97843414 − 003	.26560575 − 003
6	3	.77997083 − 004	−.76933925 − 004	11	2	−.28405458 − 003	.12641398 − 003
6	4	.35002037 − 003	.12250471 − 003	11	3	−.24615192 − 003	−.10272482 − 003
6	5	−.13743724 − 003	.16387119 − 003	11	4	−.63623344 − 003	−.49560596 − 004
6	6	−.17430947 − 003	.23906541 − 003	11	5	.45174512 − 003	.16252200 − 003
7	0	.00000000	.33996745 − 003	11	6	−.64664231 − 003	−.32202902 − 003
7	1	.70234329 − 003	−.10333474 − 003	11	7	.79107441 − 003	.68138642 − 004
7	2	.13470650 − 003	.15148079 − 003	11	8	−.12138900 − 003	.41226319 − 003
7	3	.22491632 − 003	.16358132 − 003	11	9	−.84706697 − 003	.94110576 − 003
7	4	.21646515 − 004	.35514113 − 003	11	10	−.43753163 − 003	.31800904 − 003
7	5	−.55771307 − 003	−.95395762 − 004	11	11	.11894830 − 003	−.73149258 − 004
7	6	.18515741 − 003	−.12055719 − 003	12	0	.00000000	−.38217397 − 004
7	7	.12094134 − 003	−.33484553 − 003	12	1	−.49924376 − 004	−.44181722 − 003
8	0	.00000000	.83167299 − 004	12	2	−.22977543 − 003	.66099402 − 004
8	1	−.10526624 − 003	−.39276158 − 003	12	3	−.46176757 − 004	−.28380764 − 004
8	2	−.21917685 − 003	−.97876687 − 004	12	4	−.80355593 − 004	−.25277376 − 003
8	3	.37721563 − 003	−.18299594 − 004	12	5	.35578131 − 003	−.69895511 − 004
8	4	−.37819161 − 003	.97388697 − 004	12	6	−.49640360 − 004	−.14110719 − 003
8	5	.99823643 − 004	−.49001085 − 003	12	7	.49072329 − 003	.63695662 − 004
8	6	.73546940 − 003	−.25696116 − 003	12	8	−.85966630 − 003	−.10944986 − 003
8	7	−.83167299 − 004	.57401470 − 004	12	9	.19687120 − 003	.30119493 − 003
8	8	−.18445991 − 003	.55651680 − 003	12	10	.69687695 − 003	−.65178084 − 003
9	0	.00000000	.30556565 − 003	12	11	.19084453 − 003	−.23157651 − 003
9	1	.16478072 − 003	−.16949288 − 004	12	12	−.99336138 − 005	.52016392 − 005

(5)

2	0	.00000000	.00000000	9	2	.93044507 − 004	.12964393 − 003
2	1	−.74112191 − 005	−.62970632 − 005	9	3	.14762007 − 003	.34708333 − 003
2	2	.11901684 − 007	−.28322467 − 004	9	4	−.50433862 − 003	.19845660 − 003
3	0	.00000000	−.80807796 − 004	9	5	.49908958 − 003	−.17336191 − 003
3	1	−.14477842 − 003	−.16807915 − 003	9	6	−.19263233 − 003	.79238830 − 003
3	2	−.49979542 − 004	−.16794616 − 003	9	7	−.86069764 − 003	.85997859 − 003
3	3	.16778656 − 004	−.76073172 − 004	9	8	−.16588383 − 002	.78663594 − 004
4	0	.00000000	−.15012067 − 003	9	9	.14337770 − 003	−.46960871 − 003
4	1	.11648481 − 003	.27225740 − 003	10	0	.00000000	.79698148 − 004
4	2	.24188405 − 003	.14773123 − 003	10	1	−.13651201 − 004	−.10780745 − 002
4	3	.60149357 − 004	.12236649 − 003	10	2	−.17970114 − 003	−.15463425 − 005
4	4	−.70120641 − 004	.33176345 − 004	10	3	.11680243 − 003	.71695264 − 005
5	0	.00000000	.13524954 − 003	10	4	−.35761650 − 003	−.12421006 − 003
5	1	.18212173 − 003	.14747447 − 003	10	5	.64148742 − 003	−.11468597 − 003
5	2	−.40360179 − 004	−.36030762 − 004	10	6	−.42144116 − 003	.12454076 − 003
5	3	−.45285933 − 003	−.20424588 − 003	10	7	.34504999 − 003	−.61317969 − 003
5	4	.32017405 − 003	−.20329174 − 003	10	8	.66093244 − 003	−.89552940 − 003
5	5	.14371754 − 003	−.12845128 − 003	10	9	.36350292 − 003	−.92926057 − 004
6	0	.00000000	−.26369941 − 003	10	10	−.14907853 − 003	.33836990 − 003
6	1	.23274368 − 003	.45112716 − 003	11	0	.00000000	−.17945205 − 003
6	2	−.27907566 − 004	.84738751 − 004	11	1	−.81341252 − 003	.22080898 − 003
6	3	.10932721 − 003	−.10783700 − 003	11	2	−.23614625 − 003	.10509314 − 003
6	4	.49061772 − 003	.17171282 − 003	11	3	−.20463621 − 003	−.85399363 − 004
6	5	−.19264349 − 003	.22969553 − 003	11	4	−.52892701 − 003	−.41201761 − 004
6	6	−.24432668 − 003	.33509400 − 003	11	5	.37555429 − 003	.13511122 − 003
7	0	.00000000	.41506611 − 003	11	6	−.53758034 − 003	−.26771596 − 003

Table IV (Continued)

n	*m*	Odd	Even	*n*	*m*	Odd	Even
7	1	.85749063 - 003	-.12616134 - 003	11	7	.65765268 - 003	.56646454 - 004
7	2	.16446311 - 003	.18494283 - 003	11	8	-.10091567 - 003	.34273134 - 003
7	3	.27460024 - 003	.19971637 - 003	11	9	-.70420160 - 003	.78237991 - 003
7	4	.26428221 - 004	.43359166 - 003	11	10	-.36373803 - 003	.26437399 - 003
7	5	-.68091166 - 003	-.11646865 - 003	11	11	.98886614 - 004	-.60811985 - 004
7	6	.22605861 - 003	-.14718823 - 003	12	0	.00000000	-.29263075 - 004
7	7	.14765723 - 003	-.40881276 - 003	12	1	-.38227113 - 004	-.33829961 - 003
8	0	.00000000	.90951956 - 004	12	2	-.17593914 - 003	.50612337 - 004
8	1	-.11511941 - 003	-.42952500 - 003	12	3	-.35357560 - 004	-.21731162 - 004
8	2	-.23969233 - 003	-.10703818 - 003	12	4	-.61528308 - 004	-.19354896 - 003
8	3	.41252392 - 003	-.20012480 - 004	12	5	.27242189 - 003	-.53519019 - 004
8	4	-.41359125 - 003	.10650451 - 003	12	6	-.38009643 - 004	-.10804583 - 003
8	5	.10917284 - 003	-.53587703 - 003	12	7	.37574701 - 003	.48771729 - 004
8	6	.80431110 - 003	-.28101334 - 003	12	8	-.65824681 - 003	-.83805799 - 004
8	7	-.90951956 - 004	.62774385 - 004	12	9	.15074435 - 003	.23062507 - 003
8	8	-.20172580 - 003	.60860810 - 003	12	10	.53359895 - 003	-.49906883 - 003
9	0	.00000000	.30307774 - 003	12	11	.14612973 - 003	-.17731822 - 003
9	1	.16343908 - 003	-.16811287 - 004	12	12	-.76061718 - 005	.39828971 - 005
		(6)				(7)	
2	0	.00000000	.00000000	2	0	.00000000	.00000000
2	1	-.38949694 - 004	-.33094243 - 004	2	1	-.48851532 - 004	-.41507501 - 004
2	2	.62549350 - 007	-.14884885 - 003	2	2	.78450722 - 007	-.18668938 - 003
3	0	.00000000	-.10588619 - 003	3	0	.00000000	-.98086142 - 004
3	1	-.18970985 - 003	-.22024188 - 003	3	1	-.17573498 - 003	-.20401788 - 003
3	2	-.65490504 - 004	-.22006761 - 003	3	2	-.60666182 - 004	-.20385645 - 003
3	3	.21985849 - 004	-.99682194 - 004	3	3	.20366273 - 004	-.92339159 - 004
4	0	.00000000	-.15525389 - 003	4	0	.00000000	-.12282382 - 003
4	1	.12046789 - 003	.28156697 - 003	4	1	.95304066 - 004	.22275211 - 003
4	2	.25015503 - 003	.15278275 - 003	4	2	.19790162 - 003	.12086886 - 003
4	3	.62206103 - 004	.12655069 - 003	4	3	.49212238 - 004	.10011626 - 003
4	4	-.72518345 - 004	.34310777 - 004	4	4	-.57370416 - 004	.27143801 - 004
5	0	.00000000	.12143402 - 003	5	0	.00000000	.84700212 - 004
5	1	.16351829 - 003	.13241020 - 003	5	1	.11405399 - 003	.92356095 - 004
5	2	-.36237452 - 004	-.32350279 - 004	5	2	-.25275619 - 004	-.22564316 - 004
5	3	-.40660049 - 003	-.18338250 - 003	5	3	-.28360380 - 003	-.12790927 - 003
5	4	.28746880 - 003	-.18252582 - 003	5	4	.20050945 - 003	-.12731174 - 003
5	5	.12903703 - 003	-.11533019 - 003	5	5	.90003311 - 004	-.80442794 - 004
6	0	.00000000	-.21287262 - 003	6	0	.00000000	-.13355970 - 003
6	1	.18788346 - 003	.36417458 - 003	6	1	.11788110 - 003	.22848897 - 003
6	2	-.22528518 - 004	.68405766 - 004	6	2	-.14134753 - 004	.42918875 - 004
6	3	.88254921 - 004	-.87051941 - 004	6	3	.55372553 - 004	-.54617785 - 004
6	4	.39605353 - 003	.13861600 - 003	6	4	.24849033 - 003	.86969902 - 004
6	5	-.15551239 - 003	.18542282 - 003	6	5	-.97570967 - 004	.11633725 - 003
6	6	-.19723389 - 003	.27050625 - 003	6	6	-.12374771 - 003	.16971996 - 003
		(8)				(9)	
2	0	.00000000	.00000000	2	0	.00000000	.00000000
2	1	-.21463781 - 004	-.18237052 - 004	2	1	-.11301721 - 004	-.96026918 - 005
2	2	.34468707 - 007	-.82025269 - 004	2	2	.18149445 - 007	-.43190280 - 004
3	0	.00000000	-.33666301 - 004	3	0	.00000000	-.14022323 - 004
3	1	-.60317866 - 004	-.70025463 - 004	3	1	-.25122944 - 004	-.29166248 - 004
3	2	-.20822574 - 004	-.69970055 - 004	3	2	-.86727930 - 005	-.29143169 - 004

Table IV (Continued)

n	*m*	Odd	Even	*n*	*m*	Odd	Even
3	3	.69903564 − 005	−.31693753 − 004	3	3	.29115475 − 005	−.13200739 − 004
4	0	.00000000	−.34404273 − 004	4	0	.00000000	−.11246765 − 004
4	1	.26695694 − 004	.62395260 − 004	4	1	.87268283 − 005	.20397025 − 004
4	2	.55434371 − 004	.33856669 − 004	4	2	.18121509 − 004	.11067753 − 004
4	3	.13784877 − 004	.28043642 − 004	4	3	.45062794 − 005	.91674729 − 005
4	4	−.16070070 − 004	.76032705 − 005	4	4	−.52533097 − 005	.24855109 − 005
5	0	.00000000	.19319813 − 004	5	0	.00000000	.49031225 − 005
5	1	.26015304 − 004	.21066092 − 004	5	1	.66023528 − 005	.53463060 − 005
5	2	−.57652775 − 005	−.51468390 − 005	5	2	−.14631540 − 005	−.13062022 − 005
5	3	−.64689003 − 004	−.29175643 − 004	5	3	−.16417245 − 004	−.74044068 − 005
5	4	.45735483 − 004	−.29039348 − 004	5	4	.11607083 − 004	−.73698169 − 005
5	5	.20529431 − 004	−.18348711 − 004	5	5	.52101081 − 005	−.46566693 − 005
6	0	.00000000	−.24583062 − 004	6	0	.00000000	−.48024021 − 005
6	1	.21697252 − 004	.42055790 − 004	6	1	.42386472 − 005	.82157714 − 005
6	2	−.26016495 − 005	.78996687 − 005	6	2	−.50824291 − 006	.15432327 − 005
6	3	.10191899 − 004	−.10052976 − 004	6	3	.19910293 − 005	−.19638901 − 005
6	4	.45737251 − 004	.16007722 − 004	6	4	.89349598 − 005	.31271742 − 005
6	5	−.17958959 − 004	.21413091 − 004	6	5	−.35083564 − 005	.41831352 − 005
6	6	−.22777062 − 004	.31238738 − 004	6	6	−.44495927 − 005	.61026158 − 005
		(10)				(11)	
2	0	.00000000	.00000000	2	0	.00000000	.00000000
2	1	−.32686460 − 005	−.27772584 − 005	2	1	.26631443 − 008	.22627840 − 008
2	2	.52491217 − 008	−.12491348 − 004	2	2	−.42767459 − 011	.10177383 − 007
3	0	.00000000	−.33587507 − 005	3	0	.00000000	−.60993271 − 007
3	1	−.60176696 − 005	−.69861573 − 005	3	1	−.10927794 − 006	−.12686520 − 006
3	2	−.20773840 − 005	−.69806294 − 005	3	2	−.37724278 − 007	−.12676482 − 006
3	3	.69739959 − 006	−.31619576 − 005	3	3	.12664436 − 007	−.57419603 − 007
4	0	.00000000	−.20755347 − 005	4	0	.00000000	−.16738151 − 007
4	1	.16104930 − 005	.37641700 − 005	4	1	.12987821 − 007	.30356151 − 007
4	2	.33442347 − 005	.20424990 − 005	4	2	.26969583 − 007	.16471734 − 007
4	3	.83161156 − 006	.16918117 − 005	4	3	.67065319 − 008	.13643617 − 007
4	4	−.96947229 − 006	.45868873 − 006	4	4	−.78183099 − 008	.36990955 − 008
5	0	.00000000	.65840389 − 006	5	0	.00000000	−.75187276 − 009
5	1	.88658089 − 006	.71791570 − 006	5	1	−.10124424 − 008	−.81983304 − 009
5	2	−.19647608 − 006	−.17540019 − 006	5	2	.22436838 − 009	.20030049 − 009
5	3	−.22045499 − 005	−.99428276 − 006	5	3	.25175140 − 008	.11354339 − 008
5	4	.15586290 − 005	−.98963794 − 006	5	4	−.17798963 − 008	.11301297 − 008
5	5	.69962670 − 006	−.62530951 − 006	5	5	−.79894768 − 009	.71408021 − 009
6	0	.00000000	−.45285324 − 006	6	0	.00000000	.27523617 − 008
6	1	.39969271 − 006	.77472452 − 006	6	1	−.24292614 − 008	−.47086383 − 008
6	2	−.47925901 − 007	.14552258 − 006	6	2	.29128513 − 009	−.88446043 − 009
6	3	.18774856 − 006	−.18518941 − 006	6	3	−.11411024 − 008	.11255484 − 008
6	4	.84254200 − 006	.29488388 − 006	6	4	−.51208209 − 008	−.17922519 − 008
6	5	−.33082031 − 006	.39445809 − 006	6	5	.20107158 − 008	−.23974463 − 008
6	6	−.41958429 − 006	.57545979 − 006	6	6	.25501589 − 008	−.34975426 − 008

gren, 1972; Wollenhaupt, 1972). The effect of the actual topography on the density perturbations presented in this section will be discussed later in this paper. Figure 13 shows the radial variations of the radial displacement under some mare sites. The displacements under maria Serenitatis and Imbrium are downward throughout the

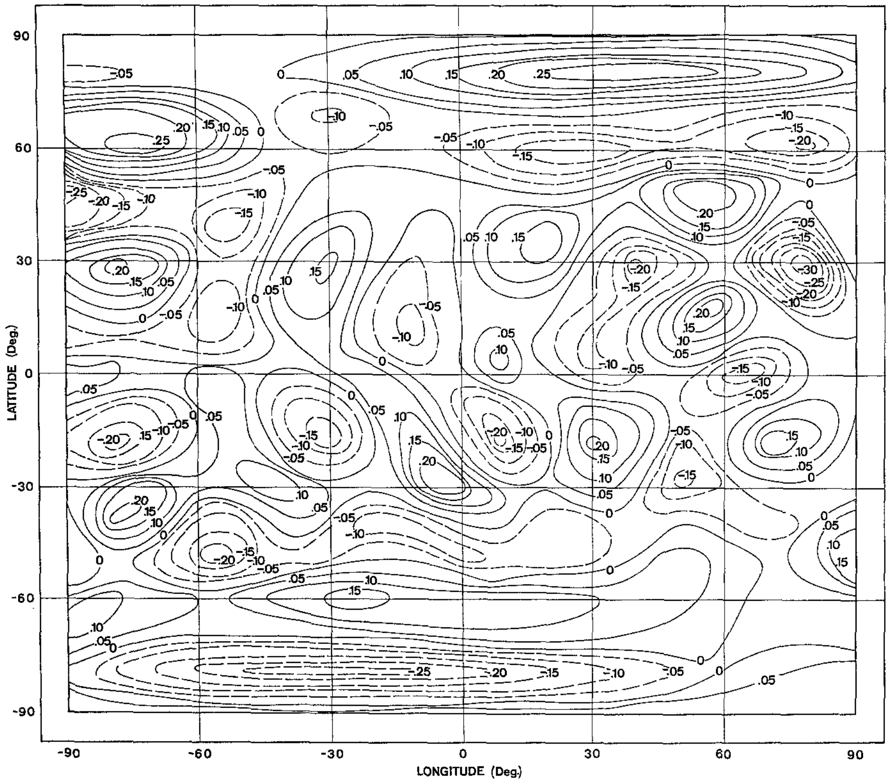

Fig. 8. Lateral variations of the density perturbations within 0–50 km depths. Units are in g cc.$^{-1}$

Moon while those under Mare Crisium are downward to a depth of about 500 km and then they become upward. This behavior is well explained in Paper I and will not be repeated here.

4. Stress Differences in the Moon

It was concluded in Paper I that there are stress differences of about 100 bars inside the Moon. The stress values were determined for a preliminary density model using the previous expression of the lunar gravitational potential, G_5. Furthermore, no consideration has been made about minimization of the shear-strain energy. The density model proposed in this paper is more realistic than the one adopted in Paper I, since allowance is made for the density perturbations to exist throughout the lunar interior and also a new updated expression is adopted for the lunar gravitational potential, G_6. Therefore, the stress differences associated with the present density model should be more realistic than those concluded in Paper I. In this section we first derive the final formula through which we determine the stress differences and then we present the lateral as well as radial variations of the stresses throughout the Moon.

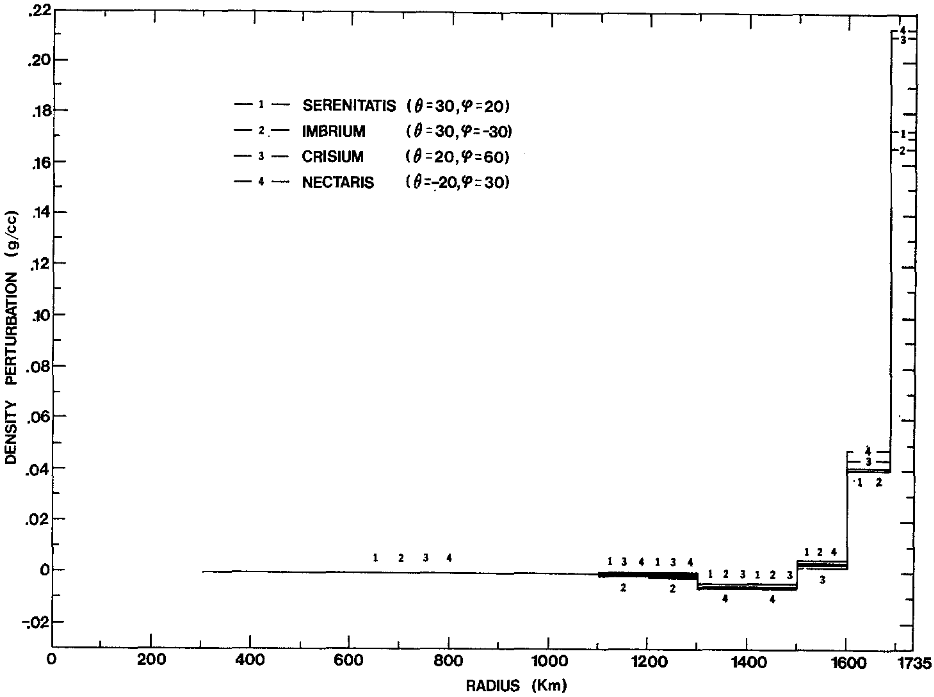

Fig. 9. Radial variations of the density perturbations under some mare sites.

The stress difference at a given point is defined by (Sokolnikoff, 1956, pp. 48–51) as

$$S = (\tau_1 - \tau_2)/2, \tag{43}$$

where τ_1 and τ_2 are the maximum and the minimum principal stresses at that point, which satisfy the following cubic equation

$$\tau^3 - \Theta_1 \tau^2 + \Theta_2 \tau - \Theta_3 = 0, \tag{44}$$

where Θ_1, Θ_2, and Θ_3 are stress invariants, i.e.

$$\Theta = T_{rr} + T_{\theta\theta} + T_{\varphi\varphi},$$

$$\Theta_2 = \begin{vmatrix} T_{rr} & T_{r\theta} \\ T_{r\theta} & T_{\theta\theta} \end{vmatrix} + \begin{vmatrix} T_{rr} & T_{r\varphi} \\ T_{r\varphi} & T_{\varphi\varphi} \end{vmatrix} + \begin{vmatrix} T_{\theta\theta} & T_{\theta\varphi} \\ T_{\theta\varphi} & T_{\varphi\varphi} \end{vmatrix},$$

and

$$\Theta_3 = \begin{vmatrix} T_{rr} & T_{r\theta} & T_{r\varphi} \\ T_{r\theta} & T_{\theta\theta} & T_{\theta\varphi} \\ T_{r\varphi} & T_{\theta\varphi} & T_{\varphi\varphi} \end{vmatrix},$$

where T_{ij} is the (i, j)th element of the stress tensor in (1, 2, 3) coordinate system. Since the invariants are independent of the coordinate system, we simply assume a spherical coordinate system (r, θ, φ). T_{ij} are determined from the stress-strain rela-

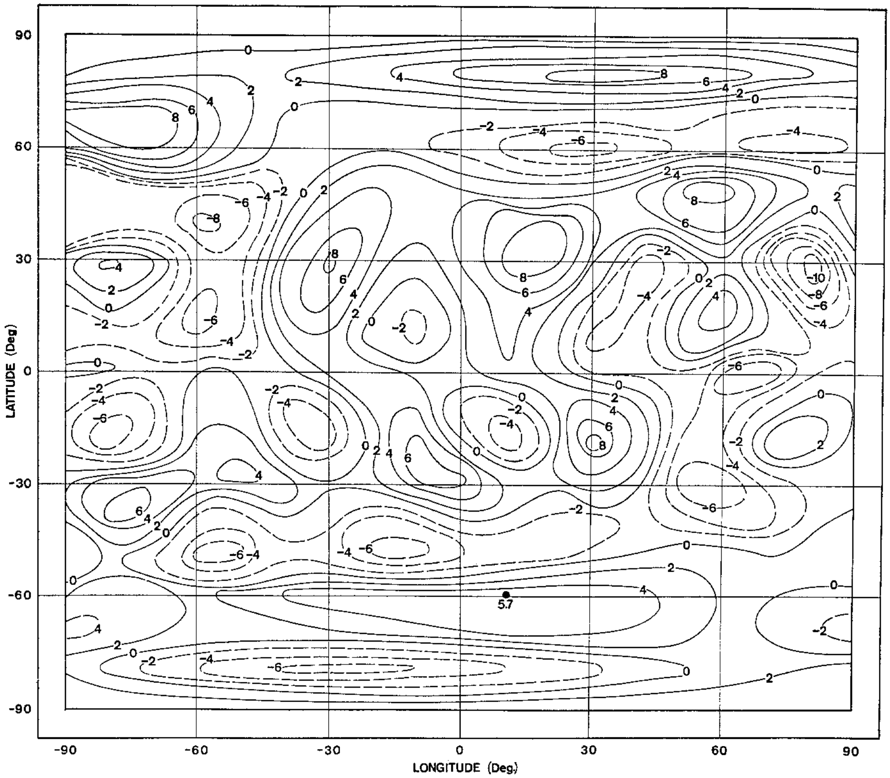

Fig. 10. Lateral variations of the gravitational potential at the surface of the Moon. This is constructed by Michael and Blackshear's, 1971, coefficients through the 12th degree harmonics. Units are in $\times 10^6$ erg. The C_{20} term is not included.

tionship,

$$T_{ij} = \lambda E_{ii}\delta_{ij} + 2\mu E_{ij}, \tag{45}$$

which is similar to Equation (7) but the hydrostatic terms are omitted. These terms add a constant quantity to the principal stresses at a given point and therefore they will be cancelled out in Equation (43). Using Equations (7), (16), (21), and (45) T_{ij} are expressed in terms of y's as

$$\begin{bmatrix} T_{rr} \\ T_{\theta\theta} \\ T_{\varphi\varphi} \\ T_{r\theta} \\ T_{r\varphi} \\ T_{\theta\varphi} \end{bmatrix} = \begin{bmatrix} 0 & R_{12} & 0 & 0 \\ R_{21} & R_{22} & R_{23} & 0 \\ R_{31} & R_{32} & R_{33} & 0 \\ 0 & 0 & 0 & R_{44} \\ 0 & 0 & 0 & R_{54} \\ 0 & 0 & R_{63} & 0 \end{bmatrix} \cdot \begin{bmatrix} y_1 \\ y_2 \\ y_3 \\ y_4 \end{bmatrix}, \tag{46}$$

where

$$R_{21} = \{2\mu(3\lambda + 2\mu)/(\lambda + 2\mu)\, r\}\, S_{nm},$$
$$R_{31} = R_{21},$$

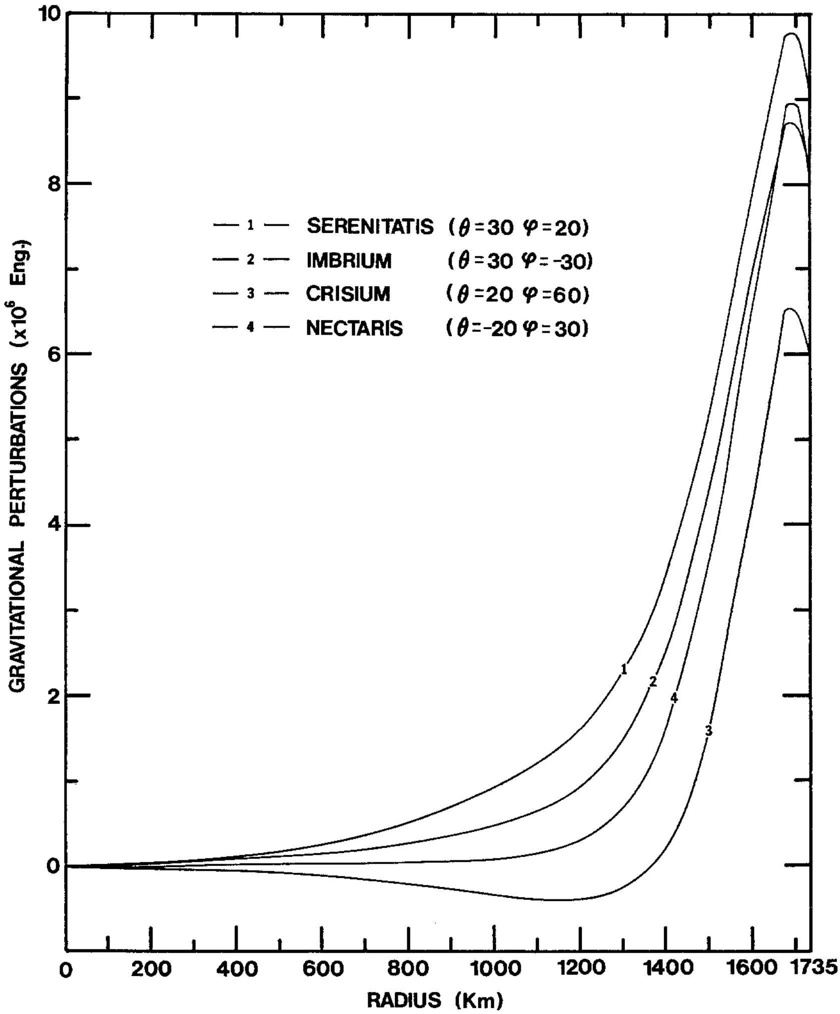

Fig. 11. Radial varations of the gravitational potential under some mare sites.

$$
\begin{aligned}
R_{12} &= S_{nm}, \\
R_{22} &= \{\lambda/(\lambda + 2\mu)\}\, S_{nm}, \\
R_{32} &= R_{22}, \\
R_{23} &= (2\mu/r)\, \{\partial^2/\partial\theta^2 - n(n+1)\,\lambda/(\lambda + 2\mu)\}\, S_{nm}, \\
R_{33} &= (-\,2\mu/r)\, \{\partial^2/\partial\theta^2 + 2n(n+1)\,(\lambda + \mu)/(\lambda + 2\mu)\}\, S_{nm}, \\
R_{63} &= (2\mu/r\sin\theta)\, \{\partial^2/\partial\theta\partial\varphi - \operatorname{cotan}\theta\cdot\partial/\partial\varphi\}\, S_{nm}, \\
R_{44} &= \partial/\partial\theta\, S_{nm},
\end{aligned}
$$

and

$$R_{54} = (1/\sin\theta)\, \partial/\partial\varphi\, S_{nm}.$$

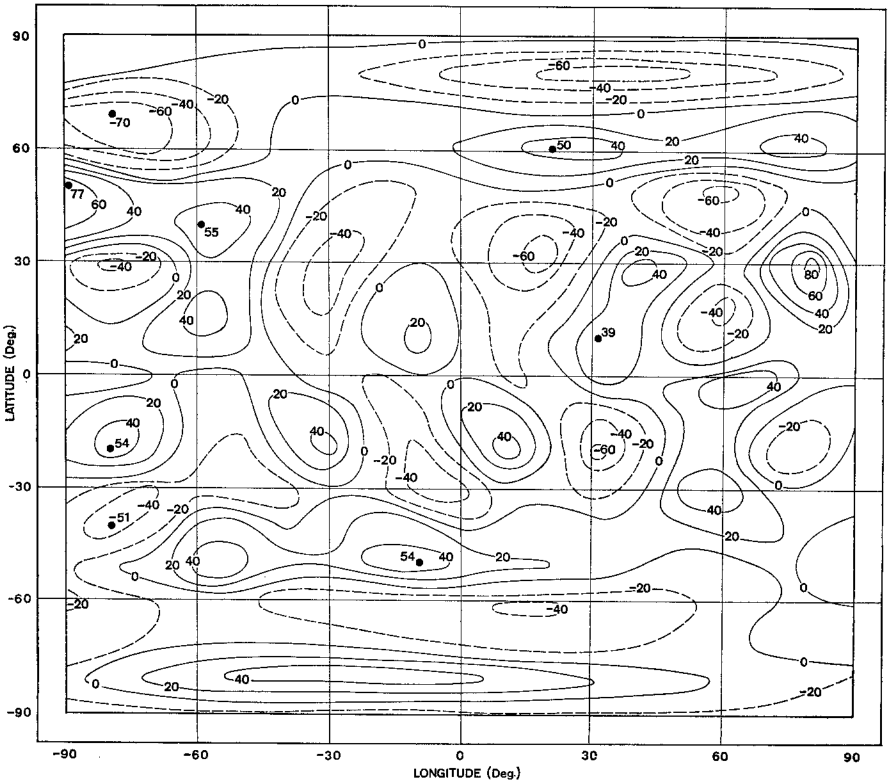

Fig. 12. Topography at the lunar surface deduced from the elastic deformation of the initial model. Units are in meters.

We determine the stress differences inside the Moon through the foregoing equations. Figure 14 illustrates the radial variations of the stress differences under some mare sites. The stresses achieve maximum values at about 250 km depth and then they decrease monotonically with increasing depth. The maximum stress differences under maria Serenitatis and Imbrium are about 70 bars, however they decrease to less than 25 bar below 600 km depth. Figure 15 displays the lateral variations of the stress differences at the radius of 1500 km. The stress differences are within 20–80 bar. In general, the circular mare regions are associated with high stress differences, while maria Procellarum and Tranquillitatis regions have low stress differences. It is worthwhile mentioning that we are dealing with anomalies whose wavelengths are larger than 800 km. Therefore, any features with smaller dimensions such as the Fra Mauro region may not be resolved from our analysis.

5. Discussion

The present section is devoted to the discussion of the effects of different phenomena on the density model presented in the previous section. The discussion leads us to a

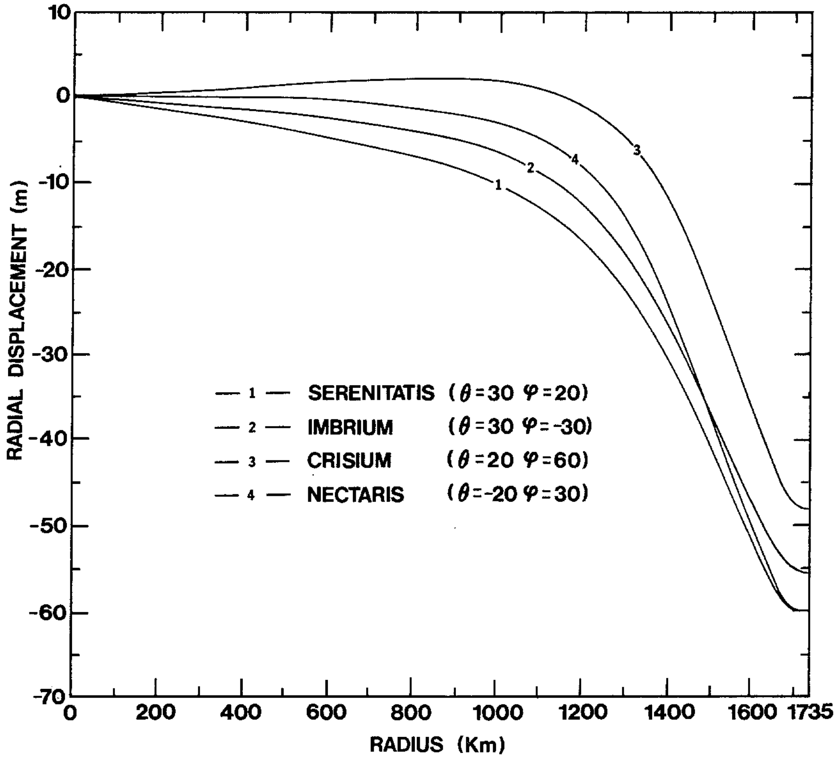

Fig. 13. Radial variations of the radial displacement under some mare sites.

somewhat realistic model of the density perturbations inside the Moon. The geophysical interpretation of the model will provide us with an estimate of the lower limit of the strength and thus the thermal conditions of the lunar interior.

A. COMPARISON WITH THE RESULTS OF PAPER I

The present density model differs from that adopted in Paper I because (1) the expressions used for the lunar gravitational potential in the two models are different and (2) in Paper I we investigated a surface layer density model, i.e. the density perturbations were confined to a surface layer of 50 km thickness, while in the present investigation the perturbations are allowed to penetrate into deep interior of the Moon. Because of the linear relationship between the density perturbations of the surface layer and the gravitational undulations it is clear from Figure 4 that density perturbations of the surface layer would have increased by a factor of about 1.5 if we had used the present expression of the gravitational potential in Paper I. For example, the density anomalies at maria Serenitatis and Imbrium would have been about 0.24 g cc^{-1} rather than about 0.16 g cc^{-1}. The associated stress differences would achieve maximum values of about 80 bar at about 180 km depth. The present density model shows density perturbations of about 0.17 g cc^{-1} at these maria sites within the surface layer. The rest of the excess mass, however, is distributed mostly within 200 km below the surface

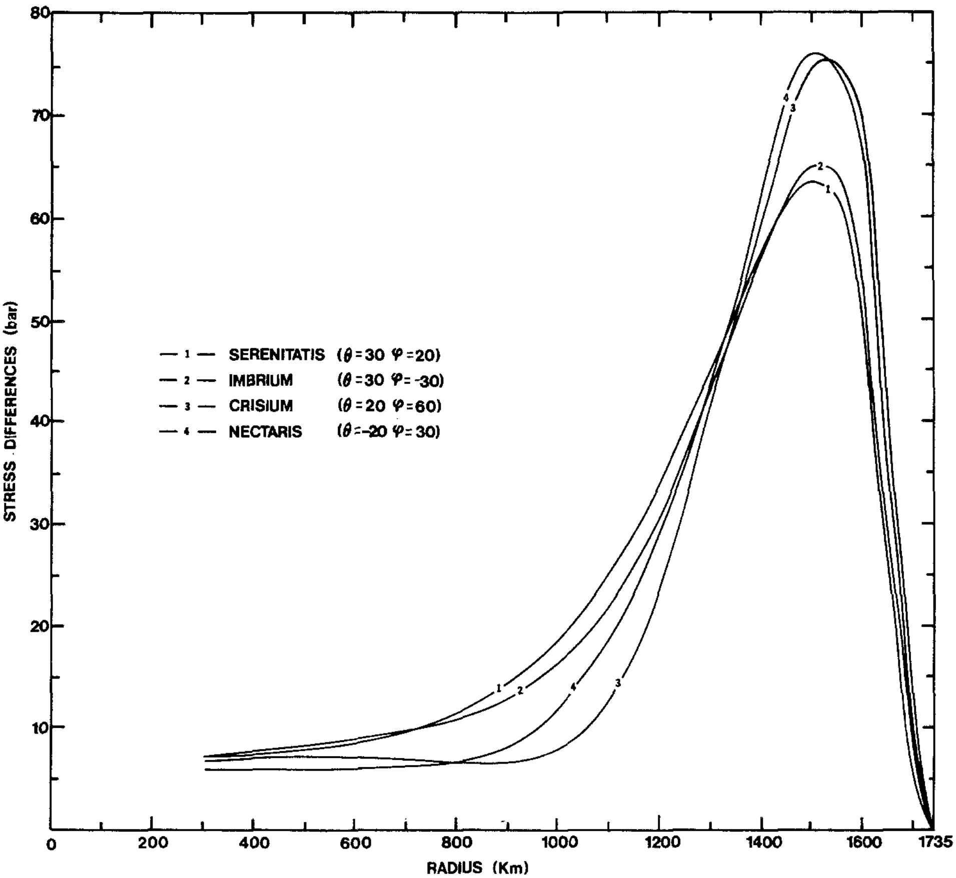

Fig. 14. Radial variations of the stress differences under some mare sites.

layer. It is clear from Figure 14 that because of this downward penetration of the density perturbations the maximum values of the stress differences do not change appreciably, however, they occur at deeper regions, about 250 km, than those associated with the surface layer model.

B. EFFECT OF A SOFT LAYER

It was pointed out in Paper I that introducing a soft layer would raise the stress differences in the layers located above the soft layer. Therefore, it would require higher strength for the upper layers. For example, if we introduce a soft layer, with rigidity about $\frac{1}{10}$ of that of the initial model, between 400 and 600 km depths, the maximum value of the stress differences would increase from about 70 bar to about 90 bar below Mare Serenitatis.

C. EFFECT OF THE SURFACE TOPOGRAPHY

Since there is no reliable spherical harmonic presentation of the surface topography

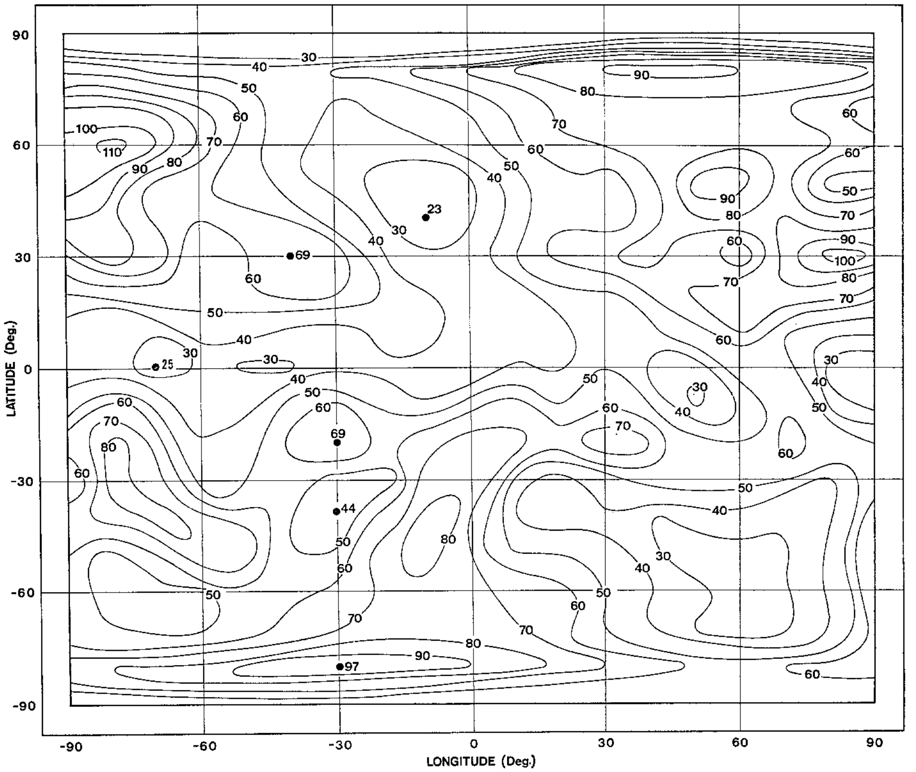

Fig. 15. Lateral variations of the stress differences at 235 km depth. Units are in bars.

of the Moon (Paper I) it is assumed in the present paper that there is no topography at the surface of the initial model. Figure 12 shows the topography which is produced at the lunar surface because of the elastic deformation of the initial model under the influence of the density perturbations. This topography is negligible in comparison with the actual topography of the lunar surface, Figure 16, deduced from the laser altimetry data of Apollo 15 (Wollenhaupt and Sjogren, 1972). To illustrate the effect of the actual surface topography on the density perturbations and their associated stress differences we consider a local feature, for example Mare Serenitatis, where reliable data are available on the surface topography. The floor of this mare is about 1.4 km below the average radius of the front side of the Moon (Arkani-Hamed, 1973c). The deficiency of the surface mass density due to this depth is about 3.7×10^5 g cm^{-2}, where the average density of the surrounding rocks is taken to be 2.8 g cc^{-1}. Using the following relationship between the surface mass density and associated gravitational potential

$$\Phi_n = \frac{4\pi G}{2n+1} (a\sigma_n),$$

where n = the degree of the spherical harmonic with a wavelength twice the diameter

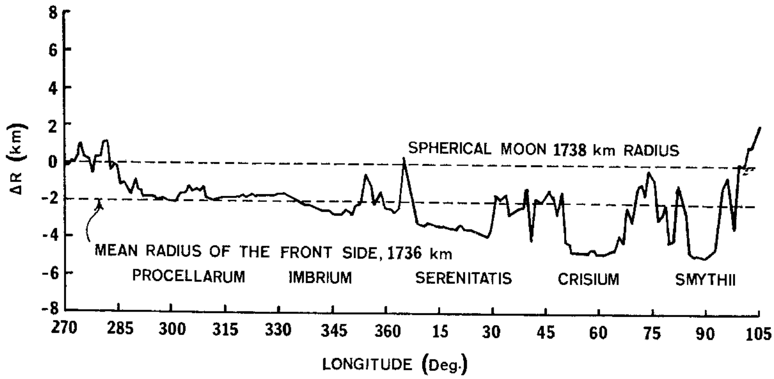

Fig. 16. Lunar surface topography deduced from Apollo 15 laser altimetry data, Wollenhaupt and Sjogren, 1972. ΔR = deviations from the mean radius of the Moon adopted in the analysis, 1738 km. The mean radius of the front side, 1736 km, is also shown in the figure.

of Mare Serenitatis, $n \approx 9$, and σ_n = the surface mass density .The gravitational potential is determined to be about -2.8×10^6 erg. This is about $\frac{1}{3}$ of the value deduced from the gravitational potential illustrated in Figure 10. Therefore, the density perturbations presented in the previous section should be increased at least by a factor of 1.3 in order to take into account the surface topography of the Moon. The resulting model is regarded as a final model which I would like to present as a density model of the Moon. This model suggests the lateral density variations of about ± 0.25 g cc^{-1} within the surface layer, 0–50 km in depth. The variations, however, reduce to about ± 0.06 g cc^{-1} and ± 0.008 g cc^{-1} within layers between 50–135 and 135–235 km, respectively. Below 235 km the perturbations are negligible. The density perturbations of the surface layer are within the variations of the measured density values of the lunar rocks. These values are listed in Table V for easy comparison. This leads us to conclude that the density perturbations of the surface layer is mainly due to the chemical and petrological variations, such as mare basalts versus highland anorthosites. The density perturbations of the deeper layers, however, can be explained by a slight chemical or temperature variation.

A factor of 1.3 increase in the density perturbations implies the same amount of increase in the associated stress differences. For example, the maximum value of the stress differences under Mare Serenitatis would increase from about 70 bar to about 90 bar at about 250 km depth.

D. STRENGTH OF THE LUNAR INTERIOR

The strength of the lunar interior can be estimated either from the extrapolation of the laboratory measurements conducted on terrestrial rocks or from the geophysical data such as the diameter-depth ratio of craters, the lateral undulations of the lunar gravitational potential, and the stress drops due to the moonquakes. The strain rates achieved in the laboratory measurements are too high in comparison to those possibly existing inside the planets such as the Moon throughout the geological time (Heard,

TABLE V

Density of the lunar rocks. References are 1 = Kanamori *et al.*, 1970; 2 = Anderson *et al.*, 1970; 3 = Stephens and Lilley, 1971; 4 = Kanamori *et al.*, 1971; 5 = Wang *et al.*, 1971; 6 = Chung, 1971; 7 = Mizutani, 1972; 8 = Todd *et al.*, 1972

Sample number		Rock type	density ($g\ cc^{-1}$)	Ref.
AS-11	10057	Basalt with void	2.88	1
	10020	Igneous – fine grained	3.18	1
	10065	Breccia – fine grained	2.34	1
	10046	Micro breccia	2.21	2
	10017	Igneous	3.10	2
	10084	Soil	2.99	2
AS-12	12002	Porous basalt	3.30	3
	12022	Porous basalt	3.20	3
	12052	Basalt-like crystalline rock	3.27	4
	12065	Basalt-like crystalline rock	3.26	4
	12002	Basalt	3.30	5
	12022	Basalt	3.32	5
AS-14	14301	Clastic	2.30	6
	14318	Clastic	2.30	6
	14321	Fragmented	2.4	6
	14311	Fragmented	2.86	7
	14313	Fragmented	2.39	7
	14310	Crystalline basalt – fine grained	2.88	8
	14377	Crystalline basalt – fine grained	2.88	8
AS-15	15418	Breccia	2.80	8
	15443	Breccia	2.80	8
	15015	Friable breccia	2.33	8
	15018	Friable breccia	2.33	8

1968). Therefore, the extrapolation of the laboratory measurements may not be valid. On the other hand the moonquakes are very small and there has been no estimate of the stress drop due to the moonquakes. Baldwin (1968) estimated the threshold strength of about 50 bar for the upper layers of the Moon, down to about 50 km, from the analysis of the diameter-depth ratios of different craters.

The foregoing discussions lead us to conclude that there are stress differences of 30–90 bar within 600 km depth below Mare Serenitatis with maximum values occurring at about 250 km depth. A very close relationship between the lunar surface topography and the maria sites implies that the lunar interior probably yielded under these stress differences. However, the lower limit for the average viscosity of the lunar interior below Mare Serenitatis is found to be 8×10^{26} poise within the last 3.3 b.y. which is the age of the final filling of the Mare (Arkani-Hamed, 1973b). Using this viscosity value we determine the stress differences as functions of time within this period through the following equation (Arkani-Hamed, 1973b)

$$\varepsilon_t = \varepsilon_{t_p} e^{(t_p - t)/\tau},$$

where ε_t is the stress difference at a given point at time t, p denotes the present values, and τ is the relaxation time. Table VI shows the values of the stress differences thus

TABLE VI

The variations of the stress differences beneath Mare Serenitatis within the last 3.3 b.y.

t (b.y. ago)	ε (bar)					
	100 km	200 km	300 km	400 km	500 km	600 km
0.0	40	90	80	65	50	35
0.5	44	99	88	72	55	38
1.0	49	110	98	80	61	43
1.5	54	122	108	88	68	47
2.0	59	133	118	96	74	52
2.5	66	149	132	107	82	58
3.0	73	164	146	119	91	64
3.3	77	173	154	125	96	67

obtained at different depths. These values are probably higher than actual ones because we have adopted the lower limit for the average viscosity. The actual stress differences are within the values of the table and the present value. It is clear from the table that stress differences of more than 100 bar have existed within 100–400 km depths of the lunar interior for 3.3 b.y. This indicates a strong lunar interior with a strength limit of about 100 bar. Such a strong medium implies that there has been no completely or partially molten layer within this region since 3.3 b.y. ago.

6. Conclusion

In this paper the lateral variations of the density of the Moon are studied. A density model is determined by solving the elastic deformation equations under the following constraints (1) the lateral undulations of the gravitational potential at the lunar surface after the deformation of the Moon under the influence of the density variations, equals to the observed potential, and (2) the shear strain energy of the whole Moon associated with its deformation achieves a somewhat minimum value. The results of this investigation indicates that:

(1) There are high positive correlations between six different spherical harmonic expressions of the lunar gravitational potential at low degree harmonics (harmonics through the 4th degree). A good agreement is also found between two successive expressions of Michael *et al.* (1969) and Michael and Blackshear (1971) for harmonics through the 12th degree. The 13th degree harmonics, however, have very different characteristics in the two expressions. This implies that the coefficients of these harmonics may not be reliable.

(2) A density model determined from elastic deformation equations with minimizing only the total shear strain energy exhibit strong oscillations with depth. These oscillations, however, vanish when we minimize the perturbations of mass in each layer together with the total shear strain energy.

(3) The model selected for the perturbations of density show strong lateral variations, ± 0.20 g cc^{-1}, within 0–50 km depth. The variations, however, decrease with depth rapidly and become negligible below 300 km depth.

(4) Including the observed surface topography of the Moon increases the density perturbations by a factor of about 1.3.

(5) The stress differences associated with the final density model are found to be on the order of 100 bar within 100–400 km depths. This indicates a strength of about 100 bar for the upper 400 km of the Moon, which has been able to support stress differences larger than this magnitude for at least 3.3 b.y.

(6) On the basis of these stress differences we conclude that there has been no completely or partially molten layer within the upper 400 km since 3.3 b.y. ago.

Appendix

In this appendix we express the integral term of the right hand side of Equation (23), $\int_\varepsilon^r \Omega_\tau^r(\overline{\overline{M}}) \cdot \bar{D}_\tau \, d\tau$, in terms of the source propagator matrix, $\overline{\overline{\Gamma}}$, and the unknown vectors $\bar{X}$. We consider two different cases; (1) when the radial variations of the density-perturbations are continuous functions of the radius, and (2) when the variations have piece wise continuous behavior.

1. Radially continuous density perturbation

In this case the unknown density perturbations, $\Delta\varrho_n(r)$, can be presented by a poly nomial function of degree K as

$$\Delta\varrho_n^{(r)} = \bar{R}^T \cdot \bar{X}, \tag{A-1}$$

where

$$\bar{R}^T = (1, r, r^2, ..., r^K),$$

and the components of the vector $\bar{X}$ are the constant coefficients of the polynomial. Using equation (A-1) the source vector, $\bar{D}$ is reduced to

$$\bar{D} = \bar{d} \cdot \bar{R}^T \cdot \bar{X} = \overline{\overline{H}} \cdot \bar{X}, \tag{A-2}$$

where

$$\bar{d} = \begin{bmatrix} 0 \\ g_o \\ 0 \\ 0 \\ 0 \\ -4\pi G \end{bmatrix},$$

and

$$\overline{\overline{H}} = \bar{d} \cdot \bar{R}^T$$

Now the integral term becomes

$$\int_{\varepsilon}^{r} \Omega_{\tau}^{r}(\overline{\overline{M}})\cdot\bar{D}_{\tau}\,\mathrm{d}\tau = \bar{\bar{\Gamma}}\cdot\bar{X} \tag{A-3}$$

and therefore

$$\bar{\bar{\Gamma}} = \int_{\varepsilon}^{r} \Omega_{\tau}^{r}(\overline{\overline{M}})\cdot\overline{\overline{H}}_{\tau}\,\mathrm{d}\tau \tag{A-4}$$

2. A LAYERED DENSITY PERTURBATIONS

In this case we assume that the lunar interior is divided into L layers and the density perturbations of each layer do not change with depth within the layer. Let the layers be numbered from the bottom to the top, i.e. the first layer is the deepest and the Lth layer is the surface layer. Furthermore, let us assume that there are no density perturbations below the jth layer. In this case, the source vector in the ith layer can be written as

$$\bar{D}_i = \bar{d}_i\cdot\Delta\varrho_{n,\,i} = \begin{cases}\overline{\overline{H}}_i\cdot\bar{X} & i \geqslant j\\ 0 & i < j,\end{cases} \tag{A-5}$$

where

$$H_{i,\,kl} = \delta_{l,i-j+1}\cdot d_{i,\,k}$$

and the components of the $\bar{X}$ vector are the density perturbations, i.e.

$$\bar{X} = \begin{bmatrix}\Delta\varrho_{n,\,j}\\ \Delta\varrho_{n,\,j+1}\\ \vdots\\ \Delta\varrho_{n,\,L}\end{bmatrix}.$$

The integral term at the top of the ith layer is

$$\int_{\varepsilon}^{r_i} \Omega_{\tau}^{r_i}(\overline{\overline{M}})\cdot\bar{D}_{\tau}\,\mathrm{d}\tau = \sum_{k=j}^{i}\bar{\bar{\eta}}(i,k)\cdot\bar{X}, \tag{A-6}$$

where the non-zero column of matrix $\bar{\bar{\eta}}(i,k)$,

$$\bar{\bar{\eta}}(i,k) = \Omega_{r_k}^{r_i}(\overline{\overline{M}})\cdot\int_{r_{k-1}}^{r_k}\Omega_{\tau}^{r_k}(\overline{\overline{M}})\cdot\overline{\overline{H}}_{\tau}\,\mathrm{d}\tau, \tag{A-7}$$

denotes the effects of the density perturbations of the kth layer on the value of the $\bar{Y}$ vector at the top of the ith layer. Equation (A-6) can be put into a more compact form as

$$\int_{\varepsilon}^{r_i} \Omega_{\tau}^{r_i}(\overline{\overline{M}})\cdot\bar{D}_{\tau}\,\mathrm{d}\tau = \bar{\bar{\Gamma}}_i\cdot\bar{X}, \tag{A-8}$$

where the source propagator, $\bar{\bar{\Gamma}}_i$, is

$$\bar{\bar{\Gamma}}_i = [\bar{\eta}_1(i,j) \vdots \bar{\eta}_1(i,j+1) \vdots \cdots \vdots \bar{\eta}_1(i,i)]. \tag{A-9}$$

and $\bar{\eta}_1$ is the non-zero column of matrix $\bar{\bar{\eta}}$.

References

Alterman, Z., Jarosch, H., and Pekeris, C. L.: 1959, 'Oscillations of the Earth', *Proc. Roy. Soc.* **A252**, 80–95.

Anderson, O. L., Scholz, C., Soga, N., Warren, N., and Schreiber, E.: 1970, 'Elastic Properties of a Micro-Breccia, Igneous Rock and Lunar Fines from Apollo 11 Mission', *Proc. of the Apollo 11 Lunar Sci. Conf.* **3**, 1959–1973.

Arkani-Hamed, J.: 1969, 'Lateral Variations of Density in the Earth's Mantle', Ph.D.thesis, MIT, Cambridge.

Arkani-Hamed, J.: 1970, Lateral Variations of Density in the Mantle, *Geophys. J. Roy. Astron. Soc.* **20**, 431–455.

Arkani-Hamed, J.: 1972a, 'Stress Differences in the Moon as an Evidence for a Cold Moon', *The Moon* **6**, 135–163.

Arkani-Hamed, J.: 1973b, 'Viscosity of the Moon. I: After Mare Formation', *The Moon* **6**, 100–111.

Arkani-Hamed, J.: 1973c, 'Viscosity of the Moon. II: During Mare Formation', *The Moon*, **6**, 112–126.

Chung, D. H.: 1972, 'Laboratory Studies on Seismic and Electrical Properties of the Moon', *The Moon* **4**, 356–372.

Gantmacher, F. R.: 1960, *The Theory of Matrices*, Vol. II, Chelsea Publishing Co.

Heard, H. C.: 1968, 'Experimental Deformation of Rocks and the Problem of Extrapolation to Nature,' *Rock Mechanics Seminar* **2**, 439–507.

Kanamori, H., Nur, A., Chung, D. H., and Simmons, G.: 1970, 'Elastic Wave Velocities of Lunar Samples at High Pressures and Their Geophysical Implications', *Proc. of the Apollo 11 Lunar Sci. Conf.* **3**, 2289–2293.

Kanamori, H., Mizutani, H., and Hamano, Y.: 1971, 'Elastic Wave Velocities of Apollo 12 Rocks at High Pressures', *Proc. of the Second Lunar Sci. Conf.* **3**, 2323–2326.

Kaula, W. M.: 1963, 'Elastic Models of the Mantle Corresponding to Variations in the External Gravity Field', *J. Geophys. Res.* **68**, 4967–4978.

Lorell, J.: 1969, 'Lunar Orbiter Gravity Analysis', *JPL Technical Report* 32–1398.

Lorell, J. and Sjogren, W. L.: 1968, 'Lunar Gravity: Preliminary Estimates from Lunar Orbiter', *Science* **159**, 625–627.

Michael, W. H., Jr. and Blackshear, W. T.: 1971, 'Recent Results on the Mass, Gravitational Field and Moments of Inertia of the Moon', *The Moon* **3**, 388–402.

Michael, W. H., Jr., Blackshear, W. T., and Gapcynski, J. P.: 1969, 'Results of the Mass and the Gravitational Field of the Moon as Determined from Dynamics of Lunar Satellites', Presented at the *12th Plenary Meeting of COSPAR*, Prague.

Mizutani, H.: 1972, 'Elastic Wave Velocities and Thermal Diffusivities of Apollo 14 Rocks', *Proc. of the Third Lunar Sci. Conf.*, in press.

Pekeris, C. L. and Jarosch, H.: 1958, 'The Free Oscillations of the Earth', in *Contributions in Geophysics*, Pergamon Press, London, 171–192.

Sokolnikoff, I. S.: 1956, *Mathematical Theory of Elasticity*, McGraw-Hill Book Co., Inc.

Stephens, D. R. and Lilley, E. M.: 1971, 'Pressure-Volume Properties of Two Apollo 12 Basalts', *Proc. of the Second Lunar Sci. Conf.* **3**, 2165–2172.

Todd, T., Wang, H., Baldridge, W., and Simmons, G.: 1972, Elastic Properties of Apollo 14 and 15 Rocks, *Proc. of the Third Lunar Sci. Conf.* ,in press.

Wang, H., Todd, T., Weidner, D., and Simmons, G.: 1971, 'Elastic Properties of Apollo 12 Rocks', *Proc. of the Second Lunar Sci. Conf.* **3**, 2327–2336.

Wollenhaupt, W. R.: 1972, 'Results from Apollo 16 Laser Altimetry', personal communication.

Wollenhaupt, W. R. and Sjogren, W. L.: 1972, 'Comments on the Figure of the Moon Based on Preliminary Results from Laser Altimetry', *The Moon* **4**, 337–347.